De Sitter space, interacting quantum field theory and alpha vacua

BY

Kevin Goldstein

B.Sc. (Hons)., University of Cape Town, 1997

M.Sc., Brown University, 2001

A DISSERTATION SUBMITTED IN PARTIAL FULFILLMENT OF THE

REQUIREMENTS FOR THE DEGREE OF DOCTOR OF PHILOSOPHY

IN THE DEPARTMENT OF PHYSICS AT BROWN UNIVERSITY

PROVIDENCE, RHODE ISLAND

May 2005

ABSTRACT OF “De Sitter space, interacting quantum field theory and alpha vacua,” BY Kevin Goldstein, Ph.D., BROWN UNIVERSITY, MAY 2004

Inspired by recent evidence for a positive cosmological constant, this thesis considers some of the implications of incorporating approximately seventy percent of the universe, namely dark energy, consistently into quantum field theory on a curved background. This may have implications for inflation, the understanding of dark energy at the present time and for introducing a positive cosmological constant into string theory. We will mainly examine various aspects of the one parameter family of de Sitter (dS) invariant states - the alpha-vacua. On the phenomenological side, such states could provide a window into trans-planckian physics through their imprint on the cosmological microwave background (CMB), and may also presently be a source of ultra-high energy cosmic rays (UHECR). From a purely theoretical perspective, formulating interacting quantum field theory in these states is a challenging problem which we consider in quite some detail.

Inflation solves many of the outstanding problems inherent to the standard model of cosmology. It also introduces the possibility that we may be able to extract information about physics at the planckian scale. During inflation, trans-planckian scales expand to macroscopic size, which might lead to an observable cosmological imprint. One way of modeling trans-planckian effects is to consider the alpha-vacua. Modeling slow-roll inflation as a transition between states with two different cosmological constants, we found that one is required to take alpha « H/M to prevent excessive particle production at the end of inflation. Here H is the Hubble constant and M is some proper momentum scale cutoff. Give these constraints we find that there may indeed be effects on the CMB.

While it was clear that there may be observable effects on the CMB, the theoretical consistency of the physics of these vacua was questioned. It was suggested that there were problems with renormalizability, locality, causality, and stability. To address these issues we sought to formulate the field theory using an imaginary-time technique We found that the theory was renormalizable with local counter-terms, and that at one-loop the renormalized stress-energy tensor was real, suggesting stability.

We found that continuing from imaginary to real time leads to an interpretation with a non-local action. The non-locality, however, relates causally separated points so it is unobservable. Unfortunately, once one couples to gravity, the non-locality may become observable - leading to instability or violations of causality.

One can also consider a real-time method where one treats the alpha-vacuum as a squeezed state with a proper momentum cut off. This state breaks dS invariance so it will eventually decay into the conventional vacuum. So, for the cut-off alpha-vacuum to have observational relevance, one may be required to fine-tune the initial conditions.

Finally, we found that the current existence of a cut off alpha-vacuum would provide a new top-down mechanism for the production of UHECR through the Unruh effect. Furthermore, we found this idea to be consistent with present observations of UHECR.

This dissertation by Kevin Goldstein is accepted in its present form by the
DEPARTMENT OF PHYSICS as satisfying the
dissertation requirement for the degree of
DOCTOR OF PHILOSOPHY

Date . . . . . .

. . . . . .
David Lowe, Advisor

Recommended to the Graduate Council

Date . . . . . .

. . . . . .
Robert H. Brandenberger, reader

Date . . . . . .

. . . . . .
Antal Jevicki, reader

Approved by the Graduate Council

Date . . . . . .

. . . . . .
Karen Newman
Dean of Graduate School and Research

The Vita of Kevin Goldstein

Born: 8 January 1973, Johannesburg, South Africa.

Education

BSc.(Hons), University of Cape Town, 1997.

Sc.M., Brown University, 2001.

Publications

K. Goldstein and D. A. Lowe, "Real-time perturbation theory in de Sitter space," Phys. Rev. D **69**, 023507 (2004).

G. L. Alberghi, K. Goldstein and D. A. Lowe, "Ultra high energy cosmic rays and de Sitter vacua," Phys. Lett. B **578**, 247 (2004)

K. Goldstein and D. A. Lowe, "A note on alpha-vacua and interacting field theory in de Sitter space," Nucl. Phys. B **669**, 325 (2003).

K. Goldstein and D. A. Lowe, "Initial state effects on the cosmic microwave background and trans-planckian physics," Phys. Rev. D **67**, 063502 (2003).

G. L. Alberghi, E. Caceres, K. Goldstein and D. A. Lowe, "Stacking non-BPS D-branes," Phys. Lett. B **520**, 361 (2001).

Preface and acknowledgments

This thesis explores some aspects of Dark Energy and interacting quantum field theory: specifically the implications of considering the implications of alpha vacua in de Sitter space.

This work is organized as follows:

Chapter 1 and Chapter 2 contain background material for that which follows. This includes a discussion of the Classical properties of de Sitter space and a short introduction to quantum field theory in curved space-time.

In Chapter 3, we focus on alpha vacua as a simple model of transplankian physics

Chapter 4 considers formulating interacting quantum field theory on the Euclidean section of de Sitter space

Chapter 5 focuses on the continuation of the Euclidean theory to the Lorentzian section and its attendant problems.

Chapter 6 considers the phenomenology of alpha vacua and ultra-high energy cosmic rays

Appendix A covers some sundry supplementary details used in the text

****

I would like to thank my advisor David A. Lowe for his help, advice and support. This work was supported in part (at Brown) by the U.S. Department of Energy under Contract FE0291ER46088-TaskA and a generous Galkin fellowship.

Dedication

For my parents, my beloved and all the meta-observers who might be out there

Conventions

The metric is has signature $(-,+,+,\ldots,+)$.

$\mathbb{M}^d$ denotes d-dimensional Minkowski space.

dS^d denotes d-dimensional de Sitter space.

Unless otherwise noted we use units with $c = \hbar = 1$

H is the Hubble constant

${}_2F_1(a,b;c;x)$ is the $(2,1)$ hypergeometric function:

$$ {}_2F_1(a,b;c;x) = 1 + \frac{ab}{1!c}x + \frac{a(a+1)b(b+1)}{2!c(c+1)}x^2 + \ldots $$

$H^{(2)}_\nu(x)$ is a Hankel function of the 2^{nd} kind defined in terms of Bessel functions:

$$ H^{(2)}_\nu(x) = J_\nu(x) - iY_\nu(x) $$

Contents

List of Figures

Chapter 1

Introduction

There exist a one complex parameter family of de Sitter invariant vacua, known as α vacua. This thesis mainly examines various aspects of these states. My inspiration for looking at these areas has been recent evidence for a positive cosmological constant which poses great theoretical challenges. I have looked α-vacua in relation to the trans-plankian problem, interacting quantum field theory and the production of ultra-high energy cosmic rays.

Inflation solves many of the outstanding problems inherent to the standard model of cosmology. It also introduces the tantalising possibility that we may be able to extract information about physics at the planckian scale. During inflation, sub-planckian scales expand to macroscopic size, suggesting that there might be an observable cosmological imprint of planckian scale physics. This trans-planckian "window of opportunity" is one of the few ways that we may be able to probe these scales (which may be governed by stringy physics) using present technology.

One way of modeling trans-planckian effects is to consider the one-parameter family of de Sitter invariant vacua. In the context of slow roll inflation, we show that all but the

Bunch-Davies vacuum generates unacceptable production of high energy particles at the end of inflation. As a simple model for the effects of trans-planckian physics, we go on to consider non-de Sitter invariant vacua obtained by patching modes in the Bunch-Davies vacuum above some momentum scale M_c, with modes in an α vacuum below M_c.

Choosing M_c near the Planck scale M_{pl}, we find acceptable levels of hard particle production, and corrections to the cosmic microwave perturbations at the level of HM_{pl}/M_c^2, where H is the Hubble parameter during inflation. More general initial states of this type with $H \ll M_c \ll M_{pl}$ can give corrections to the spectrum of cosmic microwave background perturbations at order 1. The parameter characterizing the α-vacuum during inflation is a new cosmological observable.

While it was clear that there may be observable effects on the cosmic microwave background, objections were raised about the theoretical consistency of the physics of these vacua. It was suggested that there were problems with renormalizability, locality, causality and stability for these vacua.

To address these issues we sought to formulate the field theory on the euclidean section of de Sitter space namely the sphere. We found that the euclidean theory was renormalizable with local counter-terms, and that, at one-loop, the renormalized stress-energy tensor was real suggesting stability.

Using an imaginary time formalism, we set up a consistent renormalizable perturbation theory of a scalar field in a nontrivial α vacuum. Although one representation of the effective action involves non-local interactions between anti-podal points, we argue the theory leads to causal physics when continued to real-time, and we prove a spectral theorem for the interacting two-point function. We construct the renormalized stress energy tensor and

show this develops no imaginary part at leading order in the interactions, consistent with stability.

We found that continuing from imaginary to real time leads to an interpretation with a non-local action. The non-locality, however, relates anti-podal points in de Sitter space which are inaccessible to one another so it is unobservable. Unfortunately, once one couples to gravity, the non-locality may become observable - leading one to instability or violations of causality.

One can also consider a real-time method where one treats the α vacuum as a squeezed state with a proper momentum cut off. This cut off α-vacuum breaks de Sitter invariance so it will eventually decay into the conventional vacuum. So, for the cut off vacuum to have observational relevance, one may be required to fine-tune the initial conditions.

Finally, we found that the current existence of a cut off α-vacuum would provide a new top-down mechanism for the production of UHECR through the Unruh effect. Assuming the present-day universe is asymptoting toward a future de Sitter phase, we argue the observed flux of cosmic rays places a bound on the parameter α that characterizes these de Sitter invariant vacuum states, generalizing earlier work of Starobinsky and Tkachev. If this bound is saturated, we obtain a new top-down scenario for the production of super-GZK cosmic rays. The observable predictions bear many similarities to the previously studied scenario where super-GZK events are produced by decay of galactic halo super-heavy dark matter particles.

Chapter 2

Classical de Sitter space 101

2.1 Introduction

We consider the classical properties of de Sitter space as an important preliminary to the study of quantum field theory on this background.

d-dimensional de Sitter space-time (dS) can be visualised as a hyperboloid embedded in a $(d+1)$-dimensional Minkowski space defined by the formula

$$\boxed{\eta_{AB}X^A X^B = r^2 \qquad A,B = 0\ldots d} \tag{2.1}$$

where $\eta_{AB} = \text{diag}(-1,1,\ldots,1)$ is the usual Minkowski metric. An advantage of this description is that we immediately see that dS retains the $SO(1,d)$ symmetry of the ambient Minkowski space since the left hand side of (2.1) is clearly invariant under $(d+1)$-dimensional Lorentz transformations[1]. The Hubble constant, H, which *is* actually a con-

[1]Indeed, from the higher dimension perspective, (2.1) merely describes a surface which is a constant

stant in dS, is inversely proportional to r.

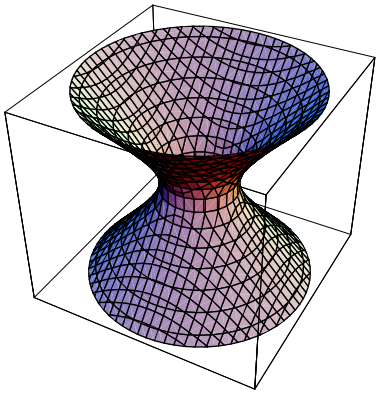

Figure 2.1: dS^2 embedded in $\mathbb{M}^3$.

De Sitter space-time is maximally symmetric and has constant positive curvature. Spaces of constant curvature are locally characterised by [63]

$$\mathbf{R}_{\alpha\beta\gamma\delta} = \tfrac{1}{d(d-1)} R \left(\mathbf{g}_{\alpha\gamma}\mathbf{g}_{\beta\delta} - \mathbf{g}_{\alpha\delta}\mathbf{g}_{\beta\gamma} \right). \tag{2.2}$$

Plugging the contraction of (2.2), $\mathbf{R}_{\alpha\beta} = \frac{1}{d} R \mathbf{g}_{\alpha\beta}$, into the contracted Bianchi identity, $\mathbf{R}^{\gamma}{}_{\alpha;\gamma} = \frac{1}{2} R_{;\alpha}$, gives $R_{;\alpha} = 0$, so, the Ricci scalar is constant.

From the contraction of (2.2), one also finds that Einstein tensor, $\mathbf{R}_{\alpha\beta} - \frac{1}{2} R \mathbf{g}_{\alpha\beta}$, is equal to $\left(\frac{1}{d} - \frac{1}{2}\right) R \mathbf{g}_{\alpha\beta}$. To satisfy Einstein's equation, either we have a cosmological constant given by $\Lambda = \left(\frac{1}{2} - \frac{1}{d}\right) R$, or the stress-energy tensor is proportional to the metric (which in turn implies the equation of state $\rho = -p$).

Good discussions of the geometry of de Sitter space dS can be found in [63, 87] on which some of the following summary is based. Other sources consulted for this chapter

proper distance from the origin that can be generated by applying Lorentz transformations to the space-like vector $(0, r, 0 \ldots 0)$.

include [6, 29, 78, 89]

In this chapter we discuss some classical properties of dS, namely – Wick rotation of the sphere to dS, various coordinate systems on dS, geodesics of dS, the Penrose diagram and causality, and finally some identifications of dS.

2.2 Analytic continuation from the sphere

dS can be obtained from a sphere by Wick rotation. We consider a sphere of radius r embedded in $\mathbb{R}^{d+1}$ defined by the formula

$$\delta_{AB}E^A E^B = r^2. \tag{2.3}$$

Performing a Wick rotations, $E^0 \to iX^0$, sends the ambient Euclidean space to Minkowski space and turns (2.3) into (2.1):

$$\delta_{AB}E^A E^B = r^2 \xrightarrow{E^0 \to iX^0} \eta_{AB}X^A X^B = r^2 \qquad A,B \in 0\ldots d \tag{2.4}$$

This Wick rotation, sends the $SO(1+d)$ symmetries of the sphere to $SO(1,d)$ which is another way of seeing what the symmetries of de Sitter space are. Usually, Wick rotation is not a very useful tool in curved space-time, but this relationship between Wick rotation and the symmetries of dS explains its utility. Some familiar geometric properties of the sphere can be carried over to de Sitter space although, a little bit of care needs to be taken since there are fundamental differences between the spaces, for example, the topology of de Sitter is $\mathbb{R} \times S^{d-1}$.

In the next section we will see how Wick rotation can be realised in a few different coordinate systems and its relationship to the symmetries of dS.

2.3 Coordinate systems

In this section we summarise some coordinate systems one may choose for dS. Depending on the problem at hand it may be helpful to use one particular coordinate set or another. Furthermore, in discussing these coordinates, certain properties of the space are elucidated. For simplicity we set $r = 1$ – the factors of r (or H) can be easily reintroduced by dimensional analysis.

Just as there are many was to skin a cat there are many ways to slice dS. Depending on how we choose to wield our cosmic cleaver we can obtain either closed, flat or open spatial sections. It is simplest to use planar sections and examples are illustrated in fig. 2.2.

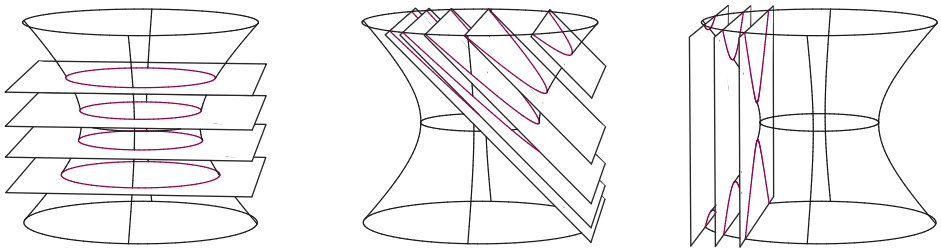

Figure 2.2: Various slicings of dS. From left to right we have closed, flat and open spatial sections.

2.3.1 Global coordinates (closed spatial sections)

Global coordinates, as their name suggests, cover all of dS. The closed spatial sections are spheres. The spatial sections start off being large in the past, contract to a minimal size at the equator, $X^0 = 0$, and then start expanding again.

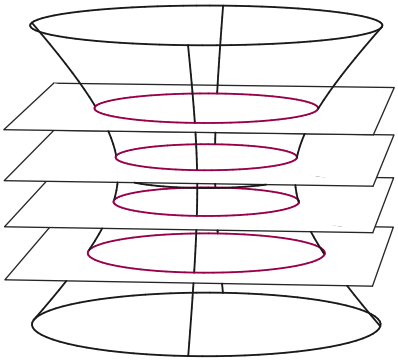

Figure 2.3: Spatial sections of global coordinates

The intersections of horizontal planes with the de Sitter hyperboloid which generate these sections are illustrated in fig. 2.3.

The time-like geodesic normals to these sections are given by the intersection of the hyperboloid with vertical planes passing though the origin as shown in fig. 2.4. The planes are related by rotations about the X^0-axis.

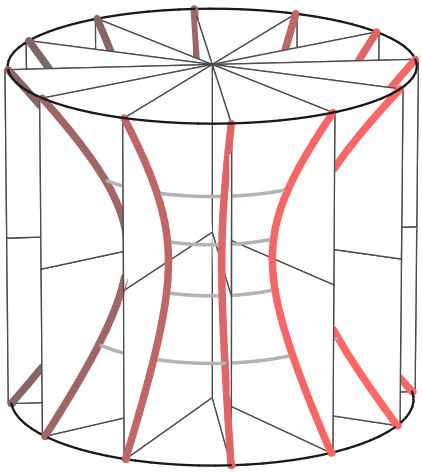

Figure 2.4: Intersection of the dS hyperboloid with vertical planes through the origin. The intersections are the geodesic normals to the spatial sections of global coordinates.

Wick rotation and global coordinates

Global coordinates are analogous to spherical polar coordinates for the d-sphere and are easily obtained from them by Wick rotation. We start with standard coordinates for the sphere

$$\begin{aligned} E^0 &= \cos\chi \\ E^1 &= \sin\chi\cos\omega_1 \\ &\vdots \\ E^{d-1} \quad 4.2 &= \sin\chi\sin\omega_1\ldots\cos\omega_{d-1} \\ E^d &= \sin\chi\sin\omega_1\ldots\sin\omega_{d-1}. \end{aligned} \tag{2.5}$$

We pick up a factor of i, by performing the transformation

$$\chi \to i\bar{t} - \pi/2, \tag{2.6}$$

since $\cos(i\bar{t} - \pi/2) = i\sinh\bar{t}$. In the new coordinate, $\bar{t}$, $E^0 = i\sinh\bar{t}$, hence the Wick rotation

$$E^0 \to iX^0, \qquad E^a \to X^a \quad a = 1 \ldots D \tag{2.7}$$

gives us the following coordinates parameterising de Sitter space

$$\boxed{\begin{array}{rcl} X^0 &=& \sinh\bar{t} \\ X^1 &=& \cosh\bar{t}\cos\omega_1 \\ &\vdots& \\ X^d &=& \cosh\bar{t}\sin\omega_1 \ldots \sin\omega_{d-1}. \end{array}} \tag{2.8}$$

It can easily be checked that (2.8) satisfies (2.1). It is also easy to see from (2.8) that planes of constant X^0 coincide with surfaces of constant $\bar{t}$.

Either by using (2.6) to transform the familiar metric for the Euclidean n-sphere,

$$ds^2 = d\chi^2 + \sin^2\chi\, d\Omega_{d-1}^2,$$

or by using (2.8) to calculate the pull back of η_{AB} on the hyperboloid (ie. plugging (2.8) into $ds^2 = \eta_{AB}dX^A dX^B$), one obtains the following expression for the metric on de Sitter space

$$\boxed{ds^2 = -d\bar{t}^2 + \cosh^2\bar{t}\, d\Omega_{d-1}^2} \tag{2.9}$$

where $d\Omega_{d-1}^2$ is the metric of a $(d-1)$-sphere.

Conformal Coordinates

Sometimes it is more convenient to express the metric with an overall conformal factor. To this end, we define a global conformal time variable, $\bar{\eta}$, by

$$d\bar{\eta}^2 = \frac{d\bar{t}^2}{\cosh^2\bar{t}} : \bar{\eta} = \int d\bar{t}/\cosh\bar{t}. \tag{2.10}$$

Choosing limits for the integral so that $\bar{\eta}$ start at 0, (2.10) gives

$$\tan\left(\tfrac{1}{2}\left(\bar{\eta} - \pi/2\right)\right) = \tanh\left(\tfrac{1}{2}\bar{t}\right). \tag{2.11}$$

Note (2.11) maps $\bar{t} \in (-\infty, \infty)$ to the finite region $\bar{\eta} \in (0, \pi)$. Plugging (2.11) and (2.10) into (2.9) gives the conformal metric

$$\boxed{ds^2 = \frac{1}{\sin^2(\bar{\eta})}\left(-d\bar{\eta}^2 + d\omega_1^2 + d\Omega_{d-2}^2\right).} \tag{2.12}$$

Symmetries and global coordinates

Another illustrative way to obtain (2.8) is by applying $SO(1,d)$ to a single point. We start with the representative point $\mathbf{e}_{(1)} = (0,1,0,\ldots 0)^T$. Applying a boost of rapidity $\bar{t}$ in the $(0,1)$-plane , gives us a time-like hyperbolic curve

$$X^A = \Big(\sinh\bar{t}, \cosh\bar{t}, 0, \ldots, 0 \Big),$$

which, is incidentally a geodesic. We then successively apply $(d-1)$ rotations to sweep out the whole space. The procedure is illustrated in fig. 2.5.

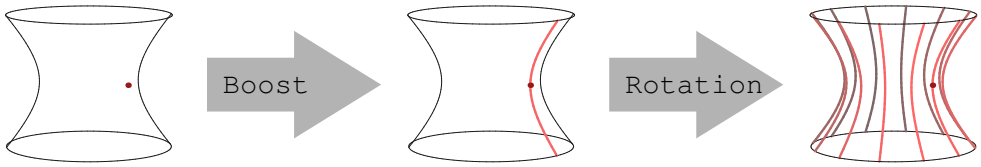

Figure 2.5: $dS = S(1,d)\cdot(0,1,0\ldots0)$

In summary, we can rewrite (2.8) more compactly, albeit less transparently, as

$$\mathbf{X}(\bar{t},\omega_1\ldots\omega_{d-1}) = M_{(d,d-1)}(\omega_{d-1})\ldots M_{(21)}(\omega_1)M_{(01)}(\bar{t})\mathbf{e}_{(1)},$$

where $M_{(AB)}$ denotes a $S0(1,d)$ rotation/boost in the (AB)-plane of $\mathbb{M}^{d+1}$. This incidentally explicitly demonstrates the transitivity of dS under its symmetry group ie. by applying group transformations to a single point we may obtain the whole space.

As previously noted the spatial sections of global coordinates start off large, contract to a minimal size at the equator and then start expanding again. This would seem to imply that the equator is some special region of de Sitter space where contraction stops and expansion begins. This in turn seems to contradict the statement that all points in dS are equivalent under $SO(1,d)$. In fact given any point in dS, we can find a new set of global coordinates where that point lies on the equator. These new coordinates will be related to our original ones by a $SO(1,d)$ transformation. Boosting the spatial sections of the old coordinates transforms them to ellipses in the new frame. Both the new and old equators will have a proper circumference of $2\pi r$. We see that the apparent specialness of the equator is a coordinate artifact. Fig. 2.6 shows the spatial sections of some boosted global coordinates.

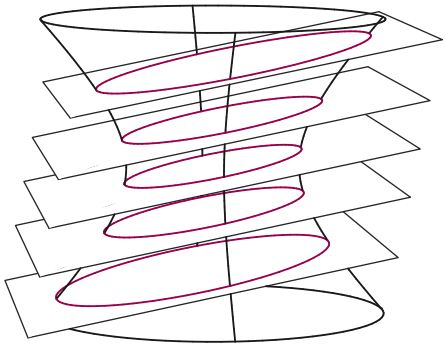

Figure 2.6: Boosted global coordinates.

2.3.2 Static coordinates

In the previous section we saw how global coordinates masked some of the symmetry of dS by making the equator seem special. The spatial sections of static coordinates are far more democratic – each spatial section corresponds to the equator in some global coordinate system. This means that the sections are equivalent under boosts. For simplicity, consider dS^2. To generate the coordinates we apply the boost $M_{(01)}(\overset{\diamond}{t})$ to an equator

$$X^A = (0, \cos\vartheta, \sin\vartheta)$$

giving us a family of ellipses all with the same proper circumference of $2\pi r$. (see fig 2.7).

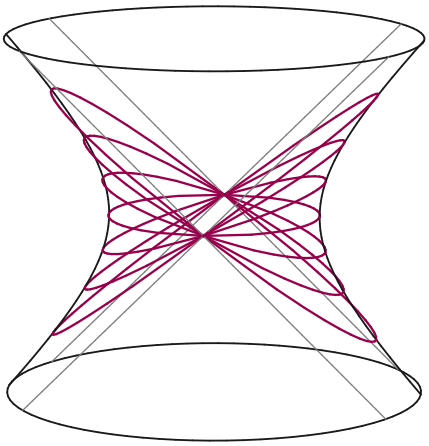

Figure 2.7: Spatial sections of static coordinates generated by boosting the equator. Notice that the spatial sections cover two spatially separated parts of dS. The grey lines denote the boundaries of static coordinates.

An advantage of static coordinates is that, as the name suggest, the metric is static. Since spatial sections are equivalent under boosts and boosts correspond to time translations, the components of the metric are time-independent. A disadvantage of static coordinates is that since we can't boost past the light cone, our coordinates will only cover half of dS. Another disadvantage is that as all the spatial sections meet at a point – so we expect a coordinate singularity there (a similar coordinate singularity arises in spherical polar coordinates at the poles). Generalising to dS^d, where the equator is $(d-1)$-sphere, we get

$$\mathbf{X}(\overset{\diamond}{t},\vartheta,\theta_1\ldots\theta_{d-2}) \;=\; M_{10}(\overset{\diamond}{t})M_{d,d-1}(\theta_{d-2})\ldots M_{32}(\theta_1)M_{21}(\vartheta)\mathbf{e}_{(1)}. \qquad (2.13)$$

Notice from fig (2.7) the family of ellipses covers two spatially separated quadrants of dS. If we would like coordinates covering just one of these regions we should just boost

half of the equator. To this end let $\rho = \sin\vartheta|_{\vartheta\in(0,\pi/2)}$and write out (2.13) explicitly to give

$$\boxed{\begin{aligned} X^0 &= \sqrt{1-\rho^2}\sinh\overset{\diamond}{t} \\ X^1 &= \sqrt{1-\rho^2}\cosh\overset{\diamond}{t} \\ X^2 &= \rho\cos\theta_1 \\ X^3 &= \rho\sin\theta_1\cos\theta_2 \\ &\vdots \\ X^d &= \rho\sin\theta_1\ldots\sin\theta_{d-2} \end{aligned}} \tag{2.14}$$

(2.14) cover just a quarter of dS - we shall see later that this region corresponds to the part of dS completely accessible to an observer.

Using (2.14) to calculate the pullback of η_{AB} gives us the metric

$$\boxed{ds^2 = -(1-\rho^2)d\overset{\diamond}{t}^2 + \frac{1}{(1-\rho^2)}d\rho^2 + \rho^2 d\Omega_{d-2}^2} \tag{2.15}$$

which is indeed static. Notice that (2.15) is reminiscent of the Schwarzschild metric and, indeed, the physics of the static patch has much in common with a black hole.

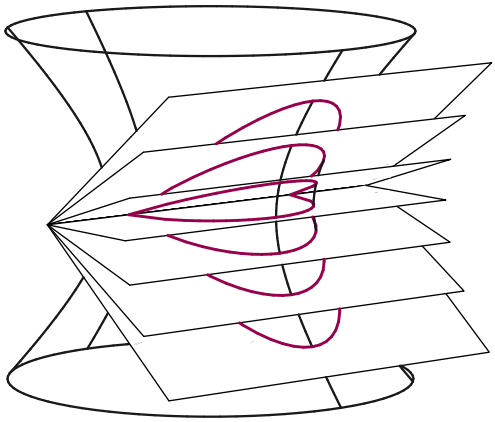

Figure 2.8: Spatial sections of the static patch. The sections are generated by the intersection of the dS hyperboloid with a family of half planes. The half planes are generated by boosting the equatorial half-plane ($X^0 = 0, X^2 > 0$) over the rapidity range $(-\infty, \infty)$.

It is easy to check that $\partial/\partial\,\overset{\diamond}{t}$ is a time-like Killing vector. As we approach $\rho = 1$, it becomes null ($\left\|\partial/\partial\,\overset{\diamond}{t}\right\|^2 = -(1-\rho^2)$) and in fact there is no globally time-like Killing vector field on dS (see section 2.4). This means that there is no globally defined concept of energy on dS.

Wick Rotation to static coordinates

We can also obtain (2.14) by Wick rotation of a different axis. Start with the following coordinates for the hemi-sphere:

$$\mathbf{E}(\vartheta, \theta_1 \ldots \theta_{d-2}, \omega) \;=\; R_{10}(\omega) R_{d,d-1}(\theta_{d-2}) \ldots R_{32}(\theta_1)\, R_{21}(\vartheta)\big|_{\vartheta\in(0,\pi/2)}\, \mathbf{e}_{(1)} \quad (2.16)$$

where R_{AB} is a $SO(d+1)$ rotation in the (AB)-plane. Perform the transformation

$$\omega \to i\overset{\diamond}{t} - \pi/2 \qquad \sin\vartheta \to \rho \tag{2.17}$$

which gives $E^1 = i\sqrt{1-\rho^2}\sinh\overset{\diamond}{t}$ so Wick rotating the E^1-axis:

$$E^1 \to iX^0 \qquad E^0 \to X^1 \qquad E^a \to X^a (a > 1) \tag{2.18}$$

gives us (2.14). Notice that Wick rotation achieves the transformation $S^d \to dS^d$ by mapping a $SO(d+1)$ rotation to a $SO(1,d)$ boost.

2.3.3 Inflationary coordinates (flat spatial sections)

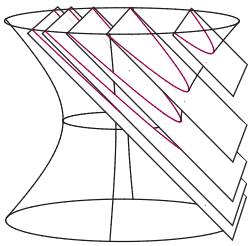

Figure 2.9: spatial sections of inflationary coordinates

Inflationary coordinates are given by

$$\boxed{\begin{aligned} X^+ &= e^{\grave{t}} \\ X^- &= e^{\grave{t}}\left(x^2 - e^{-2\grave{t}}\right) \\ X^i &= e^{\grave{t}} x^i \end{aligned}} \tag{2.19}$$

where we have used light-cone coordinates $X^{\pm} = X^0 \pm X^1$ and $x^2 = \sum_i x^i x^i$. The coordinates only cover half of the space with $X^+ > 0$ (although by using another patch with $X^+ = -e^{\grave{t}}$ we can cover the whole space). The spatial sections, generated by the intersection of the dS hyperboloid with null planes (see fig. 2.9), are flat and consist of paraboloids. They can be thought of as infinitely boosted global coordinate spatial sections and in fact (2.19) can be derived from (2.8) by appropriately taking the infinite boost limit (see 2.3.4 for details)

From (2.19) we find the inflationary metric

$$\begin{aligned} \boxed{ds^2 = -d\grave{t}^2 + e^{2\grave{t}} d\vec{x}^2} \\ = -d\grave{t}^2 + a^2(\grave{t}) d\vec{x}^2 \end{aligned} . \tag{2.20}$$

2.3.4 Conformal Coordinates

Sometimes, it will be more convenient to use conformal inflationary coordinates,

$$ds^2 = \frac{1}{\grave{\eta}^2}\left(-d\grave{\eta}^2 + d\vec{x}^2\right) = a^2(\grave{\eta})\left(-d\grave{\eta}^2 + d\vec{x}^2\right) \tag{2.21}$$

where $\grave{\eta} = \int_{\grave{t}}^{\infty} d\lambda / \exp(\lambda) = -\exp(-\grave{t})$. So $\grave{\eta} \xrightarrow{\grave{t}\to-\infty} -\infty$ and $\grave{\eta} \xrightarrow{\grave{t}\to\infty} 0$.

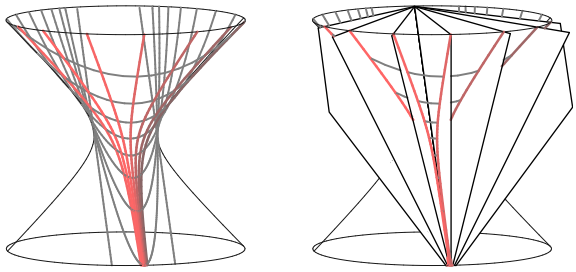

Figure 2.10: Geodesic normals to the spatial sections of inflationary coordinates are given by the intersection of the planes $X^i = \dot{x}^i X^+$ with dS .

Wick rotation to inflationary coordinates

There does not appear to be a simple way to implement Wick rotation to inflationary coordinates.

The spatial sections of inflationary coordinates lie on null planes at 45°. It is important to remember that although these planes are null with respect to the ambient Minkowski metric, the sections they generate are spatial with respect to the induced dS metric. While many useful properties of dS can be obtained by visualising it in an embedding space, this is an example where one can be misled. From the dS perspective the $SO(1,d)$ symmetry transformations do not necessarily look like boost or rotations.

Anyway, from the perspective of $\mathbb{M}^{d+1}$, Wick rotating a rotation of 45° can be interpreted as an infinite boost taking a space-like plane to a null plane. While this geometric interpretation is clear, it will cause our coordinates to blow up. Consequently one is forced to combine Wick rotation with some regularising procedure. One obvious choice ends up corresponding to Wick rotating to global coordinates and taking the appropriate infinite boost limit – so the only new element we need to discuss is how take the limit of an infinite

boost.

Taking an infinite boost

We start off with global coordinates (2.8) written in light-cone variables

$$\begin{aligned} X^+ &= \sinh\bar{t} + \cosh\bar{t}\sqrt{1-u^2} \\ X^- &= \sinh\bar{t} - \cosh\bar{t}\sqrt{1-u^2} \qquad u^2 = \sum_i u^i u^i \\ X^i &= u^i \cosh\bar{t}, \end{aligned} \tag{2.22}$$

where, $\cos\omega_1 = \sqrt{1-u^2}$ and the u^i can be read off by comparing (2.8) and (2.22). Actually (2.22) just covers half of dS since we've only taken $\cos\omega_1$ positive – as a result the boosted coordinates only cover half of dS. We apply a boost of rapidity $\bar{y}$ to (2.22):

$$X^+ \to X^+ e^{-\bar{y}} \qquad X^- \to X^- e^{\bar{y}} \qquad X^i \to X^i, \tag{2.23}$$

and take the limit as $\bar{y} \to \infty$. To get a finite answer we need to be careful about how we take the limit – taking

$$\bar{t}, \bar{y} \to \infty \qquad \bar{t} - \bar{y} \to \grave{t} \qquad u^i \to 2\grave{x}^i e^{-\bar{y}} \tag{2.24}$$

one obtains

$$\begin{aligned} X^+ &= \left(\sinh\bar{t} + \cosh\bar{t}\sqrt{1-4x^2e^{-2\bar{y}}}\right) e^{-\bar{y}} \sim e^{\grave{t}} \\ X^- &= \left(\sinh\bar{t} - \cosh\bar{t}\sqrt{1-4x^2e^{-2\bar{y}}}\right) e^{\bar{y}} \sim -e^{-\grave{t}} + x^2 e^{\grave{t}} \\ X^i &= 2x^i e^{-\bar{y}} \cosh\bar{t} \sim e^{\grave{t}} x^i \end{aligned} \tag{2.25}$$

which indeed reproduces (2.19).

2.3.5 Hyperbolic coordinates (open spatial sections)

$$\begin{aligned} X^0 &= \sinh\check{t}\cosh y \\ X^1 &= \cosh\check{t} \\ X^2 &= \sinh\check{t}\sinh y\cos\theta_1 \\ &\vdots \\ X^d &= \sinh\check{t}\sinh y\sin\theta_1\ldots\sin\theta_{d-2}. \end{aligned} \tag{2.26}$$

For completeness we include hyperbolic coordinates (2.26). They give us open spatial sections which can be generated by the intersection of dS with vertical planes as show in (2.11). As we shall see later, lines with constant spatial coordinates, (y,θ_i), are time-like geodesics.

(2.26) can be compactly written as

$$X(\check{t},y,\phi_1\ldots\phi_{d-2}) = M_{d,d-1}(\theta_{d-2})\ldots M_{32}(\theta_1)M_{02}(y)M_{01}(\check{t})\mathbf{e}_{(1)}.$$

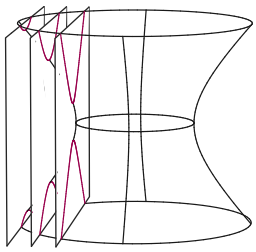

Figure 2.11: spatial sections of hyperbolic coordinates

The metric is given by

$$\boxed{ds^2 = -d\check{t}^2 + \sinh^2 \bar{t}\left(dy^2 + \sinh^2 \bar{y}\, d\Omega_{d-2}^2\right).} \tag{2.27}$$

Wick rotation

We can obtain (2.26) by Wick rotation as well. The transformation

$$\chi \to i\check{t} \qquad \omega_1 \to -iy \qquad \omega_i \to \theta_{i-1} \quad i > 1 \tag{2.28}$$

together with a Wick rotation along the E^1-axis:

$$E^1 \to iX^0 \qquad E^0 \to X^1 \qquad E^a \to X^a \quad a > 1 \tag{2.29}$$

gives us (2.26).

2.4 Geodesics and symmetry

Rather than solving any differential equations we can find the geodesics through a point of dS using its correspondence with the sphere combined with the symmetries of the space. For simplicity we consider dS^2.

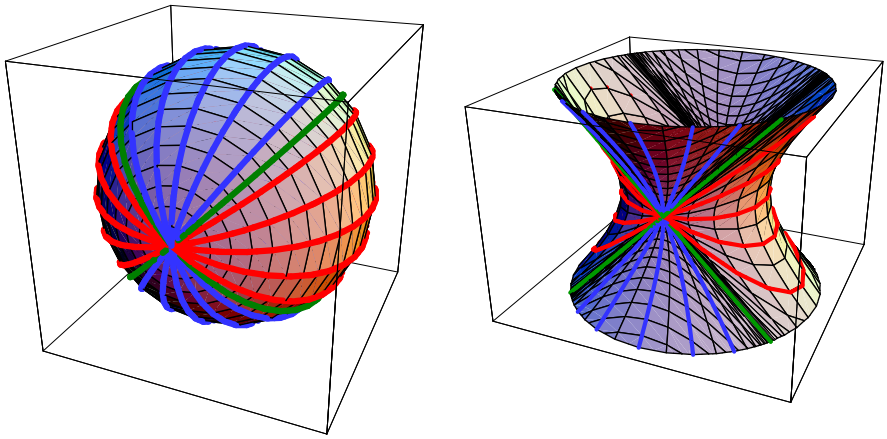

Figure 2.12: Geodesics through a point on the S^2 and on dS^2 respectively

On S^2, we can take one geodesic passing through a point and use rotations to generate all the geodesics passing through that point. The rotations are generated by a Killing field $\partial/\partial\omega$ (see fig. 2.12).

We can perform a similar procedure in de Sitter space but a little bit of care needs to be taken since $SO(1,d)$ is non-compact and the procedure is slightly more involved.

For simplicity we consider dS^2. Without loss of generality we start with the representative point $(0,1,0)$. It is easy to check that the equator $(dS \cap (0,X^1,X^2))$ is a space-like geodesic. In a repeat of what we did to generate static coordinates (2.14), we can generate the other space-like geodesics through X by boosting the equator. This gives us space-like geodesics, which are coordinate lines of constant static time, $\overset{\diamond}{t}$, related by boosts generated by the time-like Killing vector $\partial/\partial\,\overset{\diamond}{t}$. The process is illustrated in fig. 2.12 where the families of space-like geodesics are labelled in red. Similarly the "Greenwich meridian" $(dS \cap (X^0,X^1,0))$ is a time-like geodesic which we can boost to generate the family of time-like geodesics through X (labeled in blue in fig. 2.12). This is what we did to construct

hyperbolic coordinates – the time-like geodesics are coordinate lines in (2.26) with y held constant, related by boosts generated by the space-like Killing vector $\partial/\partial y$. Finally, the light-cone through X, containing null geodesics separates these two families (labeled in green in fig. 2.12).

One can now roughly see why there is no global time-like Killing field on dS. On the sphere we have the Killing field $\partial/\partial\omega$, which will be Wick rotated (2.17) to the time-like Killing field $\partial/\partial\,\overset{\diamond}{t}$ on a static coordinate patch but Wick rotated (2.28) to the space-like Killing field $\partial/\partial y$ on a hyperbolic patch.

Also, unlike the sphere, not all points in dS are joined by geodesics. There are no geodesics joining a point to points in the future light-cone or past light-cone of its antipodal point. Comparing the sphere and de Sitter space-time in fig. 2.12 we see that the geodesics which would have joined such points get blown up to infinity.

Generalising arguments of this section to higher-dimensions, one finds the geodesics of dS^d are given by the intersection of hyperplanes through the origin of $\mathbb{M}^{d+1}$ and the de Sitter hyperboloid.

2.4.1 Geodesic distance

For clarity we reintroduce factors of r in this section.

On a sphere, the geodesic distance between two points X^A and Y^A is given by

$$s = r\alpha = r\arccos(\delta_{AB}X^AY^B/r^2) \tag{2.30}$$

where $\alpha$is the angle between $X^A$and Y^A. For points that are connected by geodesics,

we can generalise (2.30) to de Sitter space by replacing δ_{AB} with η_{AB}. For those points not connected by geodesics we may use (2.30) to define a distance function by analytic continuation [6]. Rather than worry about the analytic properties of (2.30), it is sometimes more convenient just to work with is de Sitter invariant argument,

$$\boxed{Z(X,Y) := X \cdot Y / r^2}, \tag{2.31}$$

2.5 Penrose diagram

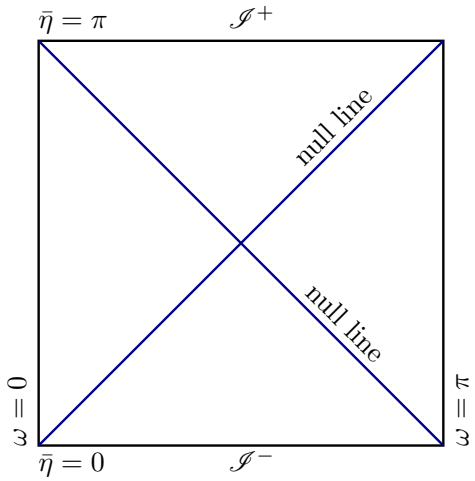

Figure 2.13: Penrose diagram of dS

As always, a Penrose diagram will facilitate understanding the the causal properties of de Sitter space. Once we've written our metric in a conformal form like (2.12), the Penrose diagram is pretty easy to construct – just throw away the conformal factor.

One sees from (2.12) that dS is conformal to a cylinder. Neglecting the overall conformal factor and projecting out all the angular variables except the first one, ω_1, leaves

behind a 2-cylinder $(0,\pi)\times S^1$ (since $\bar{\eta}\in(0,\pi)$). One may unwrap the cylinder and draw the Penrose diagram on the $(\bar{\eta},\omega_1)$-plane. By convention we only include the half range $\omega_1\in(0,\pi)$, giving us a square (as shown in fig. 2.13). On the $(\bar{\eta},\omega_1)$-plane, lines with gradient ±1 are null, since $ds^2=0\Leftrightarrow d\bar{\eta}/d\omega=\pm1$. There are space-like future and past infinities of dS "at" $\bar{\eta}=0,\pi\,\bar{t}=\pm\infty$ which we label $\mathscr{I}^{\pm}$.

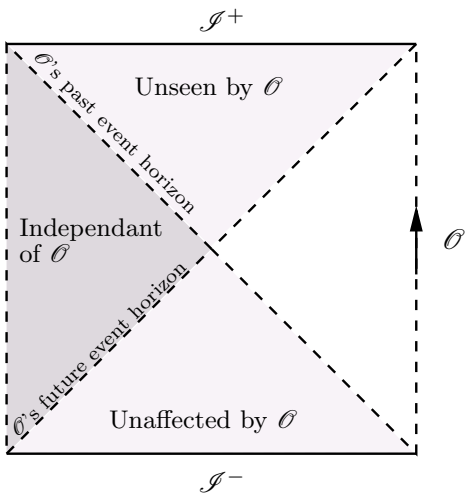

Figure 2.14: Causal structure of dS.

For any given observer, $\mathscr{O}$, dS can be broken up into four quadrants – a quadrant that $\mathscr{O}$ may both observe and influence; a quadrant that may be observed but not influenced; a quadrant that may be influenced but not observed and finally a quadrant that is completely causally separated from $\mathscr{O}$. The quadrants are defined by light-cones emanating from an observer's past and future infinities. The causal structure is illustrated in fig. 2.14.

Drawing various coordinate system on the Penrose diagram is a convenient way of see what part of dS they cover (see fig. 2.15).

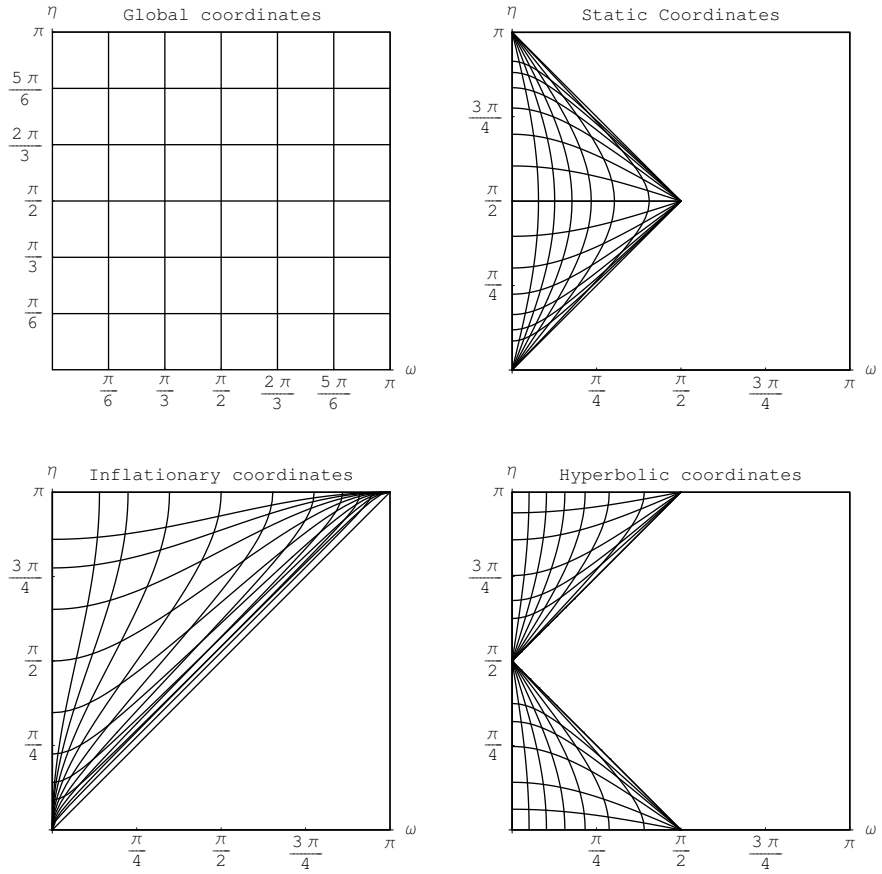

Figure 2.15: Regions of dS covered by various coordinate systems. Going clockwise from the top left corner we have: global coordinates covering the whole space; static coordinates covering the region accessible to an observer; hyperbolic coordinates covering the forward light-cone and past light-cone of an observer; and inflationary coordinates covering the patch within an observers future event horizon.

2.6 Identifications of dS

By identifying points in dS under a discrete subgroup of $SO(1,d)$ one gets a space which locally looks like dS but has a different topology.

A simple and interesting choice is elliptic de Sitter space which is the $\mathbb{Z}_2$ identification dS/A, where A consists of the identity and the antipodal transformation $X^A \rightarrow -X^A$. De Sitter originally considered elliptic de Sitter space to be more natural than dS. Recall from section 2.5 that there is a whole quadrant of dS inaccessible to an observer – as far as the observer is concerned it may as well not exist. In fact, it takes a meta-observer outside the space-time or not constrained by the speed of light to fully appreciate dS. This is where dS/A comes in – the inaccessible quadrant is precisely the region completely accessible to an antipodal observer, so identifying anti-podal points, gets rid of the problem.

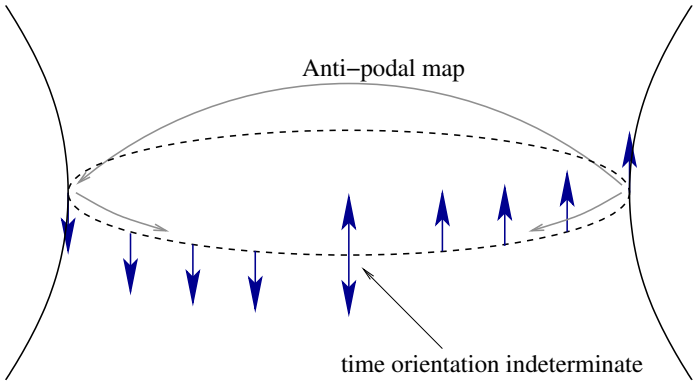

Figure 2.16: Illustration of the time-like non-orientability of Elliptic de Sitter space. There is no consistent way to assign a global time orientation.

Unfortunately elliptic de Sitter space is not time-orientable. To see why consider a time-like vector on the equator of the covering space dS as shown in fig. 2.16. Let us assign a forward time orientation to at the point on the equator. Since the anti-podal map reverses time, the equivalent anti-podal vector has opposite time-orientation. Propagating the vector and its image around the equator we reach the half-way point were the time orientation is indeterminate – it could be going either way – hence we can't assign a global time direction

to dS/A. The Penrose diagram for elliptic de Sitter is a Möbius strip (see fig 2.17).

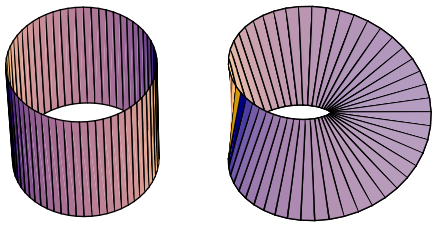

Figure 2.17: From left to right we have Penrose diagrams for dS and dS/A. Antipodal identification converts a cylinder into a Möbius strip.

Calabi and Markus who studied identifications of dS [29], found that when all points are joined by geodesics the space is not time-orientable and visa versa.

2.6.1 Causality and time-orientability in Elliptic de Sitter space

It is entertaining to consider what physics might be like in a non time-orientable space like elliptic de Sitter space. As a starting point for a gedanken experiment, it seems reasonable to require that, even if we can not assign a global direction to the arrow of time, observers can assign a local direction to the arrow of time. In other words, at least over some local space-time region, we assume an observer would perceive time going forward, entropy increasing, the rich getting richer, the poor getting poorer, etc. – just like one observes in our universe. Although this seems reasonable it will allow us to violate causality.

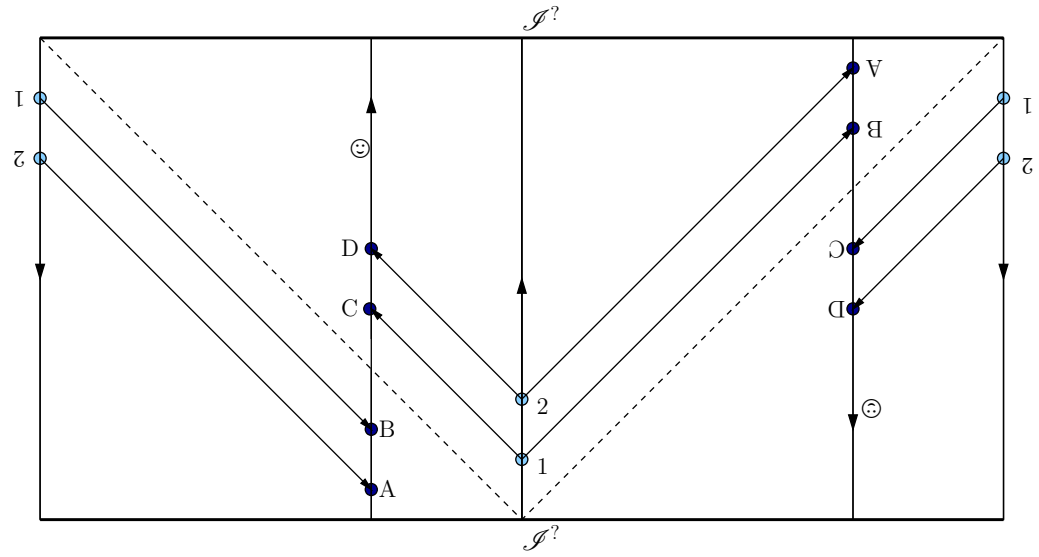

Figure 2.18: Unfolded Penrose diagram of Elliptic de Sitter space. The diagram covers the space twice. $\mathscr{I}^?$ denotes the futurepast spatial infinity. Arrows on observers' worldlines denote their local arrow of time . ☎ sends out signal 1, received by ☺ at points B and C, and signal 2, received by ☺ at points A and D.

Consider two observers (see fig. 2.18) separated by some space-like distance. Label them ☎(ET) and ☺(SETI). Suppose, that ☎ sends out two signals (1 and 2). ☺ receives the signals in the order $(2,1,1,2)$ at space-time points A, B, C and D respectively. If ☎ had sent out a movie, ☺ would initially receive it played backwards and then get it played forwards. It appears to ☺ that, at some stage, ☎ 's arrow of time flips.

Although the first set of signals that ☺ receives come from the left, ☺ will measure them as coming from the right. To see this, imagine each signal as a series of spherical electro-magnetic waves emanating from ☎. Since from ☺'s perspective the time ordering of the wave fronts is reversed, ☺ measures a spherical wave collapsing towards ☎.

Imagine that, at space-time point B, ☺, being incredibly curious, decides to go inves-

tigate the destination of these collapsing spherical waves. Traveling less than the speed of light, ☺ could reach ☎ in a finite proper time. Upon reaching ☎, ☺ and ☎ would perceive each other as travelling backwards in time. From ☎'s perspective no signal has been sent yet, while from ☺'s perspective the spherical wave has already collapsed. By talking backwards ☺ could ask ☎ to send a signal to ☺'s past. Perhaps, driven insane by years of space travel, ☺ could decide to kill ☎, preventing ☎ from sending any signals in the first place. In either case ☺ could violate causality.

So, although there are no closed time-like curves in elliptic de Sitter space, assigning a local direction to the arrow of time leads to causality violations. This is because at some stage, spatially separated observers in elliptic de Sitter space may experience the arrow of time to be facing in opposite directions.

Chapter 3

Quantum Field Theory in Curved Space-Time

3.0.2 Introduction

Without knowing how to quantise gravity, one can schizophrenically adopt a semi-classical approach, treating other fields quantum mechanically but letting them live on a classical curved background. This chimeral melding is analogous to how one might semi-classically treat atomic transitions on a classical electromagnetic background without knowing quantum electrodynamics. Since any field will have a gravitational effect, this approximation will only be valid when the quantum fields are weak enough to not significantly modify the metric and we are nowhere near the Planck scale.

Since the semi-classical approach roughly corresponds to coupling our field to some complicated potential, one might think that, although technically difficult, things should not be too conceptually different from flat space. However in a curved space time it is not

always clear which state we should choose as the vacuum – a choice which might make sense in one local inertial reference frame may look unreasonable in another, leading to observers disagreeing about what the vacuum should be. Equivalently it is not always clear that the concept of particles has global meaning on a curved background. [97]

In this chapter we consider basic canonical quantisation of a scalar field in curved space-time, some of its attendant problems and some more detailed topics which will be useful later, including the specific case of quantisation on a de Sitter background. The sections on scalar field quantisation and dS follow [19] substantially.

3.0.3 Scalar Field Quantization

For a scalar field in curved space the Klein-Gordon equation generalises to,

$$(\Box - m^2)\phi = 0, \tag{3.1}$$

where $\Box\cdot$ is the d'Alembertian,

$$\frac{1}{\sqrt{-g}}\partial_\mu\left(\sqrt{-g}\partial^\mu\cdot\right)$$

In general we can also add a term coupling to the Ricci scalar, $\xi R\phi$, giving

$$(\Box - m^2 - \xi R)\phi = 0. \tag{3.2}$$

Canonically quantisation follows a procedure familiar from flat space:

- ❖ solve the Klein-Gordon equation
- ❖ expand ϕ in a set of modes which satisfy the Klein-Gordon equation:

$$\phi(x) = \sum\!\!\!\!\!\!\int_n \left(a_n \phi_n(x) + a_n^\dagger \phi_n^*(x) \right) \tag{3.3}$$

  where $\sum\!\!\!\!\!\!\int$ denotes an sum (integral with appropriate measure) over discrete (continuous) modes

- ❖ impose canonical commutation relations

$$[a_n, a_m^\dagger] = \delta_{nm} \tag{3.4}$$

  where δ denotes the Kronendecker delta symbol (Dirac delta symbol with appropriate weighting)

For a particular set of modes, the vacuum will be defined by

$$a_n |\Omega_a\rangle = 0. \tag{3.5}$$

While the first step may involve technically difficulties, it does not present a conceptual problem. However, an ambiguity arises at the next step. Mathematically speaking, there are many possible ways to expand ϕ in terms of mode functions but different sets of modes could correspond to physically different vacuum states. This is because the different choices will in result in different annihilation operators which in turn , as we see from (3.5), result in different definitions for the vacuum state which may give us physically different

states. It is not *a priori* obvious which to choose.

While the choice of vacuum state may be suggested by a particular physical problem this is not always the case. Since we know how to do things in flat-space one could try to go to a local inertial reference frame.[1] Then we can use the state which locally looks like the Minkowskian vacuum ($|\Omega_{\mathbb{M}}\rangle$) to define the vacuum. Unfortunately, since, in general, there are no global inertial frames, the state two observers choose may be different. This means that, what looks like the vacuum at one space-time point may look like an excited state at another point.

In certain special cases, one may try use other criteria to pick out a vacuum state. In particular, if the space under consideration has special symmetries, one would expect that imposing these symmetries may fix the vacuum – just as Poincaré invariance fixes $|\Omega_{\mathbb{M}}\rangle$. dS, like flat space, is maximally symmetric, but surprisingly dS invariance does not fix the vacuum – rather one obtains a one complex-parameter family of dS invariant vacua. Another criterion one might use is to require that the Green functions have a Hadamard form.

In any case, suppose we pick a particular set of modes, then, after going through our 3 step program, we will end up with a particular choice for the vacuum.

It will be useful to define an inner product on solutions of the Klein-Gordon equation. In a globally hyperbolic space we may use the Klein-Gordon inner product

$$(\phi_1(x), \phi_2(x)) = -i \int_\Sigma \left(\phi_1 \partial_\mu \phi_2^* - \phi_2^* \partial_\mu \phi_1\right) d\Sigma^\mu \qquad d\Sigma^\mu = n^\mu \sqrt{-g_\Sigma} d^{(D-1)}\Sigma \tag{3.6}$$

[1] It may not even be possible to consider a local inertial frame given the approximation of a fixed background – we must be sure that the energy required to probe short distance doesn't affect the metric.

where Σ is a space-like Cauchy hyper-surface, g_Σ is the induced metric on Σ and n^μ is a forward pointing, time-like unit vector [19]. The Klein-Gordon inner product is sesquilinear and symmetric under complex conjugation. The symmetry of (3.6) is easily checked

$$(\phi_1, \phi_2)^* = -(\phi_1^*, \phi_2^*) = (\phi_2, \phi_1) \tag{3.7}$$

The mode functions should be complete and chosen to be orthonormal with respect to the product (3.6):

$$(\phi_m(x), \phi_n(x)) = \delta_{nm} \qquad (\phi_m^*(x), \phi_n^*(x)) = -\delta_{nm} \qquad (\phi_m^*(x), \phi_n(x)) = 0 \tag{3.8}$$

As already mentioned, from a purely mathematical perspective the choice (3.5) is not unique – we could just as easily expand ϕ in a completely different set of complete orthonormal modes, $\{\psi_n\}$,

$$\phi(x) = \sum_n \left(b_n \psi_n(x) + b_n^\dagger \psi_n^*(x), \right) \qquad [b_n, b_m^\dagger] = \delta_{nm}. \tag{3.9}$$

with the vacuum state

$$b_n |\Omega_b\rangle = 0. \tag{3.10}$$

Often one would like to investigate the relationship between various states – the classical example being adiabatic evolution of a system. Using the completeness of $\{\psi_n\}$ we may

expand a mode ϕ_n as follows

$$\phi_n = \sum\!\!\!\!\!\!\int_m (\alpha_{nm}\psi_m + \beta_{nm}\psi_m^*)\,. \tag{3.11}$$

The expansion coefficients, (α_{mn}) and (β_{mn}) are called Bogolubov coefficients. They may be found using orthonormality with respect to the Klein-Gordon inner product as follows

$$\begin{aligned} \alpha_{nm} &= (\phi_n, \psi_m) \\ \beta_{nm} &= -(\phi_n, \psi_m^*) \end{aligned} \tag{3.12}$$

Conversely, one may expand ψ_n in terms of ϕ_n,

$$\begin{aligned} \psi_n &= \sum\!\!\!\!\!\!\int_m \underbrace{(\psi_n, \phi_m)}_{=(\phi_m,\psi_n)^*}\phi_m + \underbrace{(-\psi_n, \phi_m^*)}_{=(\phi_m,\psi_n^*)}\phi_m^* \\ &= \sum\!\!\!\!\!\!\int_m \alpha_{mn}^*\phi_m - \beta_{mn}\phi_m^* \end{aligned} \tag{3.13}$$

Orthonormality imposes the following constraints on the Bogolubov coefficients:

$$\begin{aligned} (\phi_n, \phi_m) &= \delta_{nm} \;:\; \sum\!\!\!\!\!\!\int_k \left(\alpha_{nk}\alpha_{mk}^* - \beta_{nk}\beta_{mk}^*\right) = \delta_{mn} \\ (\phi_n, \phi_m^*) &= 0 \;:\; \sum\!\!\!\!\!\!\int_k (\alpha_{nk}\beta_{mk} - \beta_{nk}\alpha_{mk}) = 0 \end{aligned} \tag{3.14}$$

The Klein-Gordon inner product is also useful for finding the relationship between different sets of creation and annihilation operators which may be compactly written as the

matrix equations:

$$\begin{aligned}
\begin{pmatrix} a_n \\ a_n^\dagger \end{pmatrix} = \begin{pmatrix} (\phi, \phi_n) \\ (\phi, -\phi_n^*) \end{pmatrix} &= \int_m \begin{pmatrix} \alpha_{nm}^* & -\beta_{nm}^* \\ -\beta_{nm} & \alpha_{nm} \end{pmatrix} \begin{pmatrix} b_m \\ b_m^\dagger \end{pmatrix} \\
&= \int_m B_{nm} \begin{pmatrix} b_m \\ b_m^\dagger \end{pmatrix} \\
\begin{pmatrix} b_n \\ b_n^\dagger \end{pmatrix} = \begin{pmatrix} (\phi, \psi_n) \\ (\phi, -\psi_n^*) \end{pmatrix} &= \int_m \begin{pmatrix} \alpha_{mn} & \beta_{mn}^* \\ \beta_{mn} & \alpha_{mn}^* \end{pmatrix} \begin{pmatrix} a_m \\ a_m^\dagger \end{pmatrix} \\
&= \int_m A_{mn} \begin{pmatrix} a_m \\ a_m^\dagger \end{pmatrix}
\end{aligned} \tag{3.15}$$

As a consistency check, notice that (3.14) ensures that

$$\int_m B_{nm} A_{km} = \mathrm{diag}(\delta_{nk}, \delta_{nk}). \tag{3.16}$$

The Bogolubov coefficients relate the number of particles in a particular mode of one state relative to another state. Consider the number of excitations of a particular mode ϕ_k relative to $|\Omega_b\rangle$:

$$\begin{aligned}
N_k &= \langle \Omega_b | a_k^\dagger a_k | \Omega_b \rangle \\
&\overset{(3.15)}{=} \int_m \int_n \left\langle \left(-\beta_{km} b_m + \alpha_{km} b_m^\dagger \right) \left(\alpha_{kn}^* b_n - \beta_{kn}^* b_n^\dagger \right) \right\rangle_b \\
&\overset{(3.9,3.10)}{=} \int_n |\beta_{nk}|^2
\end{aligned} \tag{3.17}$$

The total number of particle in all modes is

$$\boxed{N = \sum\!\!\!\!\!\!\int_n \sum\!\!\!\!\!\!\int_k |\beta_{nk}|^2}. \tag{3.18}$$

3.0.4 Green's functions

To establish notation and nomenclature we define various Green's functions. The Wightman function is defined as

$$G(x,y) = \langle \Omega | \phi(x)\phi(y) | \Omega \rangle. \tag{3.19}$$

Since ϕ satisfies (3.1) (or (3.2)), G will as well, confirming that it is indeed a Green's function for the homogeneous Klein-Gordon equation. The symmetric Green's function, which can be written in terms of Wightman functions, is defined as

$$G_S(x,y) = \langle \Omega | \phi(x)\phi(y) + \phi(y)\phi(x) | \Omega \rangle = G(x,y) + G(y,x) \tag{3.20}$$

The Feynman propagator, defined as a time ordered expectation value, is given by

$$\begin{aligned} iG_F(x,y) &= \langle \Omega | \mathscr{T}\left(\phi(x)\phi(y)\right) | \Omega \rangle \\ &= \theta_{xy} G(x,y) + x \leftrightarrow y \end{aligned} \qquad \theta_{xy} = \begin{cases} 1 & x^0 > y^0 \\ 0 & x^0 < y^0 \end{cases}. \tag{3.21}$$

Since $\Box\theta \sim \delta$, G_F satisfies the inhomogeneous Klein Gordon equation.

Depending on the vacuum, we may get different Green's functions. For example, we

get different mode sums for the Wightman functions

$$\begin{aligned} G^a(x,y) &= \langle \Omega^a | \phi(x)\phi(y) | \Omega^a \rangle \\ &= \sum_n \phi_n(x)\phi_n^*(y) \end{aligned} \tag{3.22}$$

and

$$\begin{aligned} G^b(x,y) &= \langle \Omega^b | \phi(x)\phi(y) | \Omega^b \rangle \\ &= \sum_n \psi_n(x)\psi_n^*(y) \end{aligned} . \tag{3.23}$$

3.0.5 Quantum field theory in de Sitter space

Having discussed the general formalism we can consider a scalar field on dS. We will find the Euclidean of Bunch-Davies vacuum state. Since they will be relevant later, we shall use conformal planar coordinates (4.2). This case is mathematically simpler than most since we have flat spacial sections (although one should remember that these coordinates only cover half of dS). We will follow the procedure discussed in 3.0.3 albeit with some of the gory details filled in (except for simplicity we set the Hubble constant to one – $H = r^{-1} = 1$). Finally, we will show how to obtain the family of de Sitter invariant states – the α-vacua.

The firsts step is to solve (3.1) in the coordinate system, (4.2). Given the ansatz,

$$\phi_k = \frac{e^{i\vec{k}\cdot\vec{x}}}{(2\pi)^{\frac{3}{2}} a(\grave{\eta})} \chi_k(\grave{\eta}), \tag{3.24}$$

(3.1) leads to

$$\chi_k'' + \left(k^2 + \frac{M^2}{\grave{\eta}^2} \right) \chi_k = 0 \tag{3.25}$$

with

$$M^2 = m^2 + \left(\zeta - \frac{1}{6}\right) R. \tag{3.26}$$

Note that M^2 is not necessarily positive. Also since R (see 2.1) is constant in dS, M is a constant. The general solution is

$$\chi_k(\grave{\eta}) = \frac{1}{2}\sqrt{\pi\grave{\eta}}\, H_\nu^{(2)}(k\grave{\eta}) \equiv \chi_{Ek}(\grave{\eta}) \tag{3.27}$$

together with its complex conjugate. $H_\nu^{(2)}(x)$ is a Hankel function of the second kind and $\nu = \frac{9}{4} - \frac{m^2}{H^2} - 12\zeta = \frac{1}{4} - M^2$. The appearance of the flat space mode function, $e^{i\vec{k}\cdot\vec{x}}$, is no coincidence since, as previously mentioned, we have chosen a coordinate system with flat spacial sections.

It may be checked that we have found a complete set of orthonormal functions satisfying (3.1). Given this set, the next step is to define a Fock space by expanding in the our field in terms of the mode functions

$$\hat{\phi} = \sum\!\!\!\!\!\!\int_k \phi_k(\grave{\eta}) a_k + \phi_k^*(\grave{\eta}) a_{-k}^\dagger \tag{3.28}$$

and imposing canonical commutation, (3.4). We may also define a Fock vacuum state by taking the field operator and demanding $a_k|\Omega\rangle = 0$. The symmetric Green's function $\langle\phi(x)\phi(y) + \phi(y)\phi(x)\rangle_\Omega$is given by a mode sum

$$G_S(x,y) \quad = \quad \sum\!\!\!\!\!\!\int_k \left(\phi_k(x)\phi_k^*(y) + \phi_k(y)\phi_k^*(x)\right) \tag{3.29}$$

Performing the mode sum [26] one finds that the symmetric Green's function is a $(2,1)$-hypergeometric function –

$$G^E(x,y) = 2c\ {}_2F_1(h_+,h_-;2;\frac{1+Z}{2}) \tag{3.30}$$

where

$$h_\pm \equiv \frac{3}{2} \pm i\mu, \qquad \mu \equiv \sqrt{m^2 - \left(\frac{3}{2}\right)^2}, \qquad c \equiv \frac{\Gamma(h_+)\Gamma(h_-)}{(4\pi)^2}, \tag{3.31}$$

and $Z = X \cdot Y$ is the dS invariant defined in the previous chapter 2.31.

We see that (3.30) is invariant under the $SO(1,d)$ symmetries of dS. The dS invariant vacuum state which gives us this Green's function is called the Bunch-Davies or Euclidean vacuum – hence the superscript E in (3.30). As is the case for the Minkowskian Green's function, (3.30) is singular when the points x and y are null related (ie. when $Z = 1$).

As noted in [6,78] and as we shall see in the next section this is not the only dS invariant Fock space vacuum state one can obtain.

A family de Sitter invariant vacua

Since performing mode sums can be quite technical it may be easier to obtain the Green's functions directly by noting that they satisfy the Klein-Gordon equation themselves. In order to obtain dS invariant answers one can recast the equations of motion in terms of the

invariant Z [6, 53] as

$$\left((Z^2-1)\frac{d^2}{dZ^2} + 4Z\frac{d}{dZ} + m^2 \right) G(Z) = 0. \tag{3.32}$$

While (3.30) is a dS invariant solution to (3.32) there is another solution –

$$ {}_2F_1(h_+, h_-; 2; \frac{1-Z}{2}). \tag{3.33}$$

which has the property that it is singular when the antipodal point of x is null related to y (ie. when $Z = -1$). The most general dS invariant solution is a linear combination of (3.30,3.33). Working backwards one can find the Bogolubov transformation which relates the mode functions of a general alpha state to the Euclidean one (see 5.1). The possible linear combinations give us a one (complex) parameter family of vacua. Since α has been used to parameterise the states, they have been dubbed α-vacua. We will discuss them in much more detail later.

Chapter 4

Alpha-vacua and transplankian physics

4.1 Introduction

Inflation magnifies quantum fluctuations at fundamental length scales to astrophysical scales, where their imprint is left on the formation of structure in the universe. In conventional slow roll inflation, the universe undergoes an expansion of at least 10^{26} during the inflationary phase. With such a huge expansion factor, modes which give rise to observable structures apparently started out with wavelengths much smaller than the Planck length. This is the so-called trans-planckian problem in inflation [22, 23, 76, 77, 90] .

In the past year, there has been much debate about whether potential modifications to physics above the Planck scale could actually be observed [42,44,24,21,74,34,43,33,68,79, 71,91] . By considering the local effective action at the Hubble scale H (which we will take to be $10^{13} - 10^{14}$ GeV), [68] has argued that trans-planckian corrections to the spectrum of cosmic microwave background perturbations could at best be of order $(H/M_{pl})^2$ which is typically far too small to be observed in conventional inflationary models. However others

[42, 44, 24, 21, 74, 34, 43, 33] have obtained a correction of order H/M_{pl} by considering a variety of methods for modeling trans-planckian effects. Such a correction is potentially observable in the not too distant future.

In this chapter, based on [54], we represent the effect of trans-planckian physics simply by allowing for nontrivial initial vacuum states for the inflaton field, which we treat as a free scalar field moving in a de Sitter background. The most natural vacuum states to consider are the de Sitter invariant vacuum states constructed by Allen and Mottola [6, 78]. The vacuum states are known as α-vacua. We find these all lead to infinite energy production at the end of inflation, with the exception of the Bunch-Davies (Euclidean) vacuum state.

We go on to consider non-de Sitter invariant vacuum states constructed by placing modes with comoving wavenumber $k > M_c a(\eta_f)$ in the Bunch-Davies vacuum, where $a(\eta_f)$ is the expansion factor at the end of inflation. Modes with $k < M_c a(\eta_f)$ are placed in a non-trivial α vacuum. These states have a particularly simple evolution in de Sitter space – the length scale at which the patching occurs simply expands as the scale factor grows. Many more complicated initial states asymptote to such states as the universe expands.

For M_c of order M_{pl} it is possible to find initial states that do not overproduce hard particles, and produce corrections to the cosmic microwave background spectrum at order H/M_c in agreement with [44]. For $H \ll M_c \ll M_{pl}$ there are initial states that produce corrections to the spectrum at order 1.

In [34,33] an initial state was constructed by placing modes in their locally Minkowskian vacuum states as the proper wavenumber passed through the scale of new physics M_c. This turns out to be a special case of the class of initial states we consider. To avoid large back-reaction problems in this case, we show the condition $M_c \ll M_{pl}$ must hold. This condition

is rather easy to satisfy. Our more general initial states may be viewed in a similar way as an initial state that puts modes in a k-independent Bogoliubov transformation of the locally Minkowskian vacuum as proper wavenumber passes through the scale M_c.

4.2 General setup

We will conduct our analysis using linearized perturbation theory in a de Sitter (dS) background. Planar coordinates covering half of dS, with flat spacial sections, result in the metric

$$ds^2 = -dt^2 + e^{2Ht} d\vec{x}^2 = dt^2 + a^2(t) d\vec{x}^2 \tag{4.1}$$

It will be more convenient to use conformal coordinates, giving

$$ds^2 = \frac{1}{(\eta H)^2}\left(-d\eta^2 + d\vec{x}^2\right) = a^2(\eta)\left(-d\eta^2 + d\vec{x}^2\right) \tag{4.2}$$

where $\eta = \int_t^\infty dt'/a(t') = -\exp(-Ht)/H$. So $t \to -\infty$ and $\eta \to -\infty$, and $t \to \infty$ as $\eta \to 0$.

Klein-Gordon Equation in curved space is

$$\left(\Box + m^2 + \zeta R\right)\phi = 0 \tag{4.3}$$

for a scalar field with mass m and non-minimal coupling to R given by ζ. In momentum space we can solve this equation by defining

$$\phi_k = \frac{e^{i\vec{k}\cdot\vec{x}}}{(2\pi)^{\frac{3}{2}} a(\eta)} \chi_k(\eta) \tag{4.4}$$

which leads to

$$\chi_k'' + \left(k^2 + \frac{M^2}{H^2\eta^2}\right)\chi_k = 0 \tag{4.5}$$

with

$$M^2 = m^2 + \left(\zeta - \frac{1}{6}\right)R \tag{4.6}$$

so M^2 is not necessarily positive. The general solution is

$$\chi_k(\eta) = \frac{1}{2}\sqrt{\pi\eta}\,H_\nu^2(k\eta) \equiv \chi_{Ek}(\eta) \tag{4.7}$$

together with its complex conjugate, where $\nu = \frac{9}{4} - \frac{m^2}{H^2} - 12\zeta = \frac{1}{4} - M^2$.

Such a complete set of orthonormal modes may be used to define a Fock vacuum state by taking the field operator

$$\hat{\chi} = \sum_k \chi_k(\eta)a_k + \chi_k^*(\eta)a_{-k}^\dagger \tag{4.8}$$

and demanding $a_k|0\rangle = 0$. As shown by Allen [6] and Mottola [78], the general family of de Sitter invariant vacuum states can be defined using the modes

$$\chi_k = \cosh\alpha\,\chi_{Ek}(\eta) + e^{i\delta}\sinh\alpha\,\chi_{Ek}^*(\eta) \tag{4.9}$$

with $\alpha \in [0,\infty)$ and $\delta \in (-\pi,\pi)$. $\alpha = 0$ is the Bunch-Davies vacuum (a.k.a. Euclidean vacuum).

For a massless minimally coupled scalar, this solution takes a particularly simple form

$$\chi_{Ek}(\eta) = \frac{e^{-ik\eta}}{\sqrt{2k}}\left(1 - \frac{i}{k\eta}\right) \tag{4.10}$$

As discussed in [6] this case gives rise to difficulties in canonical quantization, and there is no de Sitter invariant Fock vacuum. Nevertheless, we will use this simple example in the following with the understanding a small mass term could be added to eliminate this problem, and the expressions we derive will not be substantially changed.

We will need to extract two physical quantities from the expression (4.9). The first is the number of particles produced in the mode k defined with respect to the $\alpha = 0$ vacuum. This is simply equal to

$$n_k = \sinh^2 \alpha \tag{4.11}$$

This will be a good approximation to the number of particles produced at the end of inflation, when a transition is made to a much more slowly expanding universe, provided the wavelength of the modes in question are much smaller than the Hubble radius. This follows simply from the fact that at high wavenumber, the wave equation for χ_k reduces to that of flat space, so we can approximate the final geometry by Minkowski space. We wish to count particles with respect to the Lorentz invariant vacuum state, which corresponds to the $\alpha = 0$ vacuum in this regime.

The second physical quantity of interest is the contribution of this mode to the spectrum of CMBR perturbations. We compute this by examining $|\phi_k(\eta)|^2$ in the distant future

$\eta \to 0$ for the massless scalar (4.10). The contribution is then

$$P_k = \frac{k^3}{2\pi^2 a^2}|\chi_k|^2 = \left(\frac{H}{2\pi}\right)^2 |\cosh\alpha - e^{i\delta}\sinh\alpha|^2 \tag{4.12}$$

4.3 Initial state effects

We begin by reviewing what happens for the usual Bunch-Davies vacuum, $\alpha = 0$. Clearly the particle production at high frequencies (4.11) vanishes. Fluctuations in the scalar field modes mean different regions of spacetime expand at slightly different rates, which gives rise to density perturbations after inflation has ended. The amplitude of these perturbations are frozen in as these modes expand outside the Hubble radius during inflation, and become density perturbations once they reenter the horizon after the end of inflation. For $\alpha = 0$, $P_k = (H/2\pi)^2$ is independent of k and hence scale invariant. When one allows for the detailed shape of the inflaton potential, H becomes effectively k dependent, leading to small deviations from the scale invariant spectrum of perturbations, which in general are highly model dependent.

For a nontrivial $\alpha \neq 0$ vacuum we immediately see a problem. At the end of inflation there will be a large amount of particle production at wavelengths smaller than the Hubble radius (4.11). Since this production is independent of k [6], this will lead to an infinite energy density, and singular backreaction on the geometry. We conclude then that at wavelengths below some scale, the modes must be in a local $\alpha = 0$ vacuum state.[1] Actually, α

[1] [51] also concludes that only the Euclidean vacuum smoothly patches onto the Lorentz invariant Minkowski vacuum, in the context of two-dimensional de Sitter space. They also point out that for all $\alpha \neq 0$ the vacuum state picks up a nontrivial phase under de Sitter isometries, which cancels in expectation values.

need not be exactly zero for the high wavenumber modes. We will return to this point at the end of this section.

Nevertheless, we can still consider initial states that involve modes in an $\alpha \neq 0$ state, provided their wavelengths are sufficiently large. Perhaps the simplest such initial state is to place modes at some fixed conformal time η_0 in the $\alpha = 0$ state for $k > M_c a(\eta_f)$ where η_f is the conformal time at the end of inflation, and M_c is some scale at which physics changes, and we have in mind taking $M_c \gg H$. Modes for $k < M_c a(\eta_f)$ can be placed in an $\alpha \neq 0$ state.

In order that the particle production at the end of inflation be irrelevant versus the energy stored in the inflaton, we must have

$$M_c^4 \sinh^2 \alpha \ll \Lambda = \frac{3M_{pl}^2 H^2}{4\pi} \tag{4.13}$$

where M_{pl} is the Planck mass.[2] If we saturate this bound, $\sinh \alpha \sim HM_{pl}/M_c^2$. The correction to the CMBR spectrum P_k(4.12) will then be of order HM_{pl}/M_c^2. This is linear in H in agreement with the estimates of [42, 44, 34] and is potentially observable. Of course, since we have done the computation in pure de Sitter space, the effect appears as a k-independent modulation of the $\alpha = 0$ result, which on its own would require an independent determination of H to measure directly. However, in inflation H is actually slowly changing, which will translate into k-dependence of H, and hence α. This will show up as k-dependent corrections to the cosmic microwave background spectrum P_k which are potentially more

[2]This condition is necessary to avoid large back-reaction on the geometry. It would also be interesting to consider the limit when this energy is not irrelevant, and to use this particle production as a source for reheating.

easily distinguishable from the $\alpha = 0$ case [42, 43].

To obtain an upper bound on the size of the correction to the CMBR spectrum, we can imagine taking M_c to be much smaller than M_{pl}, which is certainly plausible. This allows α to be of order 1, and still consistent with negligible hard particle production (4.13). This limit will lead to corrections to the CMBR spectrum (4.12) at order 1.

4.3.1 Transition at proper energy M_c

Now let us consider a more detailed model for the initial state where we assume the initial condition is fixed due to some change in physics at the proper energy scale M_c. Let us review the computation of [34, 33]. The essential idea was to note the α-vacuum satisfying

$$\begin{aligned} \cosh\alpha &= e^{i(\gamma-\beta)}\frac{2\beta-i}{2\beta} \\ e^{i\delta}\sinh\alpha &= e^{i(\gamma+\beta)}\frac{i}{2\beta} \end{aligned} \tag{4.14}$$

with $\beta = M_c/H$ and γ real, can be interpreted as an initial state which places modes in their locally Minkowskian vacuum as the proper wavenumber k/a passes through the scale M_c. This is seen by noting that at time $\eta = -M_c/Hk$ the field ϕ_k (with χ_k given by 4.9) satisfies $\pi_k = -ik\phi_k$ where π_k is the conjugate momentum. Such a relation is satisfied by the Lorentz invariant vacuum in Minkowski space. One may also interpret the state at time $\eta = -M_c/Hk$ as a minimum uncertainty state [34] .

For sufficiently large k, the above prescription does not apply, because the relevant time η will be after the end of inflation. These modes may safely be placed in the Bunch-Davies vacuum.

This initial state is a special case of the type described above. High frequency particle

creation at the end of inflation gives an energy density of order $M_c^4 \sinh^2 \alpha$. Since here $\sinh \alpha \sim H/M_c$, we require

$$M_c^2 H^2 \ll M_{pl}^2 H^2 \tag{4.15}$$

This will hold whenever $M_c \ll M_{pl}$, which is easy to satisfy. This condition was also obtained in [42] .

Note that the general class of initial states described above may be reinterpreted in the same way as states arising from a boundary condition placed at a fixed proper energy scale. Rather than imposing the condition that the initial state corresponds to a locally Minkowski vacuum as the wavenumber k/a passes through M_c, one instead demands the mode be in a general k-independent Bogoliubov transformation of the locally Minkowski vacuum. This corresponds to a generic boundary condition at the scale M_c that is independent of time. In this way, modes are placed in a nontrivial α-vacuum when $k/a(\eta_f)$ at the end of inflation is below the scale M_c. Higher k modes will remain in the Bunch-Davies vacuum. This is precisely the type of state we described above.

It is interesting to view this boundary condition in the context of the nice slice argument of [75] used to define effective field theory in a curved background. The conformal time slicing (4.2) satisfies the criteria for a "nice slicing". This mean we may define fields with, for example, a spatial lattice cutoff on proper wavelengths below $1/M_c$. As one moves forward on these time slices, the proper wavelength of a given mode (4.7) expands, so new modes descend from above the cutoff scale, and we assume these are placed in their ground state. The main difference with asymptotically flat space, is that we now have the option of placing these modes in one of the nontrivial de Sitter invariant α-vacua. Any other choice

would lead to continuous creation of particles at the cutoff scale which would cause drastic back-reaction on the geometry.

Provided interacting quantum field theory in de Sitter is consistent in a general α vacuum, there seems to be no dynamics that prefers one value of α over another. Only when we patch de Sitter space onto standard cosmology at the end of inflation do we generate observable consequences of the α parameter in the form of extra particle production, and imprint on the CMBR. In the context of slow roll inflation, we should therefore regard the value of α during inflation as a new cosmological observable which encodes information about trans-planckian physics.

At the end of inflation we make a transition from the de Sitter geometry to a standard cosmological geometry. To describe the UV cutoff in this more general context, we need to replace the simple α-vacuum suitable for de Sitter, by a boundary condition fixed by some more general dynamical condition such as the locally Minkowskian boundary condition of [34,33] described above (4.14). The effective value of α will then change as the effective value of H changes. Note for us H determines the vacuum energy density, and is not related to the Hubble parameter outside the de Sitter phase. In the limit that the cosmological constant becomes very small (the effective H decreases by a factor of 10^{-30} or so to match with today's vacuum energy density), we make a smooth transition to a $\alpha \sim 10^{-30} H/M_c$ boundary condition at the cutoff scale after the end of inflation. If we regard the present state of the universe as a de Sitter phase with very small cosmological constant, this type of boundary condition does not lead to continuous particle creation, so is not subject to the constraints explored in [91].

The value of α during inflation may be selected by local physics at Planckian energies,

but in general α may also be influenced by the initial state of the universe. This initial state is not necessarily completely determined by physics at Planckian energies. For example the initial state may emerge as a special state of very high symmetry as a result of dynamics on much higher energy scales, which will leave their imprint on the value of α in the de Sitter phase.

Chapter 5

Interacting quantum field theory and alpha vacua I

A common problem in formulating quantum field theory on a curved background is the ambiguity in the choice of the vacuum. As already mentioned, in de Sitter space there is a one-parameter family of vacua invariant under the de Sitter group, which have been dubbed the α vacua [30, 93, 78, 6]. These vacua are perfectly self-consistent in the context of free theories. It has long been suggested that the only physically sensible vacuum is the Euclidean (a.k.a. Bunch-Davies) vacuum.

One reason for this choice is that the free propagators in the Euclidean vacuum exhibit a Hadamard singularity, which matches with what is expected in the flat space limit [70, 97]. However the physical motivation for restriction to Hadamard singular propagators is obscure in the context of interacting quantum field theory, and certainly nothing appears to go wrong with the α-vacuum propagators at the free level. In particular, as shown in [6] the commutator Green function is vanishing at spacelike separations in an α-vacuum and

in fact is independent of α.

The Green functions in a nontrivial α vacuum exhibit singular correlations between anti-podal points. Of course since the commutator is compatible with locality this does not lead to acausal propagation of information. However some authors have suggested that once interactions are included the α-vacua do not lead to a sensible perturbative expansion of Green functions. Banks et al. [12] have argued non-local counter-terms render the effective action inconsistent. Einhorn et al. [45] have argued that α vacuum correlation functions are non-analytic and conclude that they are physically unacceptable. Related arguments are made in Kaloper et al. [67], who argue that because an Unruh detector is not in thermal equilibrium in an α vacuum, thermalization will lead to decay to a Euclidean vacuum.

This issue has direct bearing on the theory of inflation. The conventional view of inflation places the inflaton in the Euclidean vacuum. However, as emphasized in [34, 33, 54] , the initial conditions for inflation may place the inflaton in a non-trivial α-vacuum, see also [85] for earlier work in this direction. This has a potentially large effect on the predictions for the CMB spectrum, see for example [34, 33, 54, 15] and references therein. Furthermore, if there is a residual value of α today, there are many interesting predictions for other observable quantities such as cosmic rays, that we consider in more detail in chapter 7.

In, this chapter, based on [55], we show in an imaginary time formulation the α-vacua do indeed have a well-defined perturbative expansion, that yields finite renormalized amplitudes in a conventional manner. This goes a long way to refuting some of the objections raised in [12, 45, 67], see also [35] for discussion of consistency of α-vacua.

We begin in section 2 by reviewing the free field results of [30, 93, 78, 6]. In particular, the α-vacuum may be regarded as a squeezed state created by a unitary operator U acting on the Euclidean vacuum. This idea will be central to the formalism we develop. This leads to a generalized Wick's theorem, which allows us to expand any free α-vacuum Green function in terms of products of Euclidean vacuum two-point functions. In section 3 we describe the interacting theory in an imaginary time formalism. In particular, in the interaction picture, we show that the effective Lagrangian becomes non-local when U is commuted through the fields. We show that UV divergences in amplitudes satisfy a non-trivial factorization relation which relates the coefficients of local counter-terms to non-local ones. Once local counter-terms are fixed, non-local terms are completely determined, which implies the theory is renormalizable in the conventional sense. In section 4 we outline how to continue the imaginary time amplitudes to real time. We carry this through in detail for the interacting two-point function, and prove a spectral theorem in this case. One immediate consequence is that even in the interacting theory, the expectation value in an α-vacuum of the commutator of two fields vanishes at spacelike separations, as required for causality of local observables. In section 5 we use the Green function to define a renormalized stress energy tensor, and we conclude in section 6.

5.1 Free fields

Let us begin by reviewing the construction of the α-vacua [6, 78, 30, 93]. As mentioned in dS space there is a one complex-parameter family of the dS invariant vacua, dubbed the alpha vacua, $|\alpha\rangle$. One of these, the Euclidean or Bunch-Davies vacuum, $|E\rangle$, is defined

by using mode functions obtained by analytically continuing mode functions regular on the lower half of the Euclidean sphere. The Euclidean modes can be chosen such that $\phi_n^E(x)^* = \phi_n^E(\bar{x})$, where $\bar{x}$ is the antipode of x, ($\bar{x} \equiv -x$). See, for example, [78, 20] for explicit expressions of these mode functions.

The modes of an arbitrary α-vacuum general are related to the Euclidean ones by a mode number independent Bogoliubov transformation,

$$\phi_n^\alpha = N_\alpha(\phi_n^E + e^\alpha \phi_n^{E*}) \tag{5.1}$$

where $N_\alpha \equiv (1 - \exp(\alpha + \alpha^*))^{-\frac{1}{2}}$ and we require that $\mathrm{Re}(\alpha) < 0$. The Euclidean vacuum corresponds to $\alpha = -\infty$.

In terms of creation and annihilation operators

$$b_n = N_\alpha(a_n - e^{\alpha *} a_n^\dagger) \tag{5.2}$$

where b and a are operators satisfying (3.5) with respect to the α-vacuum and Euclidean respectively. This transformation can be implemented using a unitary operator

$$b_n = \mathscr{U} a_n \mathscr{U}^\dagger \tag{5.3}$$

where

$$\mathscr{U}_\alpha \equiv \exp(\sum_n c_\alpha a_n^{\dagger 2} - c_\alpha^* a_n^2) \tag{5.4}$$

$$c_\alpha \equiv \frac{1}{4}\exp(-i\mathrm{Im}(\alpha))\log\tanh(-\mathrm{Re}(\alpha)/2) \tag{5.5}$$

and we use the standard Taylor expansion of the exponential to define the ordering. The vacua are related by

$$|\alpha\rangle = \mathscr{U}_\alpha |E\rangle \tag{5.6}$$

since

$$b_n \mathscr{U}\,|E\rangle = \mathscr{U}\,a_n|E\rangle = 0\,. \tag{5.7}$$

From this perspective the α-vacuum may be viewed as a *squeezed state* on top of the usual Euclidean vacuum.

5.1.1 Generalized Wick's theorem

The Fock space built on the α vacuum is not unitary equivalent to that of the Euclidean vacuum in general, because the unitary transformation mixes positive and negative frequencies. However, as far as quantum field theory in a fixed de Sitter background goes, this unitary transformation leaves the complete set of physical observables invariant. For our purposes, we take these observables to be finite time Green functions, from which one may obtain S-matrix elements as described in [36, 19]. All this unitary transformation does is to mix these observables up in a non-local way, as we explain in more detail later in this section. This is the underlying reason that the interacting α-vacuum theory is consistent.

If we were only considering the ϕ field on its own this would be the end of the story. However if we wish to view ϕ as the inflaton, physics dictates that ϕ should be locally

coupled to other fields. Thus we are interested in correlators of the field ϕ with respect to the α vacuum. The conjugated field $\mathscr{U}\phi(x)\mathscr{U}^\dagger$ on the other hand, would yield correlators in the α-vacuum identical to the usual Euclidean vacuum correlators of ϕ, but would be coupled non-locally to other fields.

Since the unitary transformation involves modes of arbitrarily high frequency (up to some physical cutoff) the systematics of renormalizable perturbation theory will be quite different from the usual Euclidean vacuum perturbation theory [3, 4, 38, 40, 39, 41]. It will be our goal in the rest of this paper to elaborate on renormalizable perturbation theory in the α-vacuum.

The correlators of interest take the form of expectation values of products of fields ϕ with respect to the state $|\alpha\rangle$, or equivalently as conjugated fields $\tilde{\phi} \equiv \mathscr{U}^\dagger\phi\mathscr{U}$ with respect to $|E\rangle$

$$\begin{aligned}\langle\alpha|\phi(x_1)\phi(x_2)\dots\phi(x_n)|\alpha\rangle &= \langle E|\mathscr{U}^\dagger\phi(x_1)\mathscr{U}\mathscr{U}^\dagger\phi(x_2)\mathscr{U}\mathscr{U}^\dagger\dots\mathscr{U}\mathscr{U}^\dagger\phi(x_n)\mathscr{U}|E\rangle \\ &= \langle E|\tilde{\phi}(x_1)\tilde{\phi}(x_2)\dots\tilde{\phi}(x_n)|E\rangle\ .\end{aligned} \tag{5.8}$$

Now, letting $\gamma = e^\alpha$ (so that $|\gamma| < 1$),

$$\begin{aligned}\tilde{\phi}(x) &= \mathscr{U}^\dagger\phi(x)\mathscr{U} \\ &= \mathscr{U}^\dagger\left(\sum_n \phi_n^\alpha(x)b_n + \phi_n^{\alpha*}(x)b_n^\dagger\right)\mathscr{U} \\ &= \sum_n \phi_n^\alpha(x)a_n + \phi_n^{\alpha*}(x)a_n^\dagger \\ &= N_\alpha\sum_n \left(\phi_n^E(x) + \gamma\phi_n^E(\bar{x})\right)a_n + \left(\phi_n^E(x) + \gamma\phi_n^E(\bar{x})\right)^* a_n^\dagger \\ &= N_\alpha\left(\phi_0(x) + \phi_1(x)\right)\end{aligned} \tag{5.9}$$

where we have defined

$$\phi_0(x) \equiv \phi(x) \ , \qquad \phi_1(x) \equiv \sum_n \gamma \phi_n^E(\bar{x}) a_n + \gamma^* \phi_n^{E*}(\bar{x}) a_n^\dagger \tag{5.10}$$

If γ is real, then $\tilde{\phi}(x)$ is simply a linear combination of $\phi(x)$ and $\phi(\bar{x})$. For γ complex this isn't quite true, but the additional phases are simple to keep track of.

Using these relations we can express any α-vacuum correlator in terms of a sum of Euclidean vacuum correlators, giving us a generalized Wick's theorem. The simplest example is

$$\begin{aligned} \langle \alpha | \phi(x)\phi(y) | \alpha \rangle &= N_\alpha^2 \left(G_E(x,y) + |\gamma|^2 G_E(\bar{x},\bar{y}) + \gamma G_E(\bar{x},y) + \gamma^* G_E(x,\bar{y}) \right) \\ &\equiv G_\alpha(x,y) \end{aligned} \tag{5.11}$$

where $G_E(x,y) \equiv \langle E | \phi(x)\phi(y) | E \rangle$ is the Wightman function on the Euclidean vacuum. It is convenient to introduce a two index notation,

$$G_\alpha(x,y) = \sum_{i,j=0,1} G_{ij}(x,y) \tag{5.12}$$

where

$$\begin{aligned} G_{00}(x,y) &= N_\alpha^2 G_E(x,y) \ , & G_{10}(x,y) &= N_\alpha^2 \gamma G_E(\bar{x},y) \ , \\ G_{01}(x,y) &= N_\alpha^2 \gamma^* G_E(x,\bar{y}) \ , & G_{11}(x,y) &= N_\alpha^2 |\gamma|^2 G_E(\bar{x},\bar{y}) \end{aligned} \tag{5.13}$$

which we will use later.

The Wightman function diverges when x and y are null separated. As we can see from

(5.11), for the α-vacua, there are additional divergences when one point is null separated with the antipode of another. This feature has led many to consider the α-vacua unphysical [45, 12, 67].

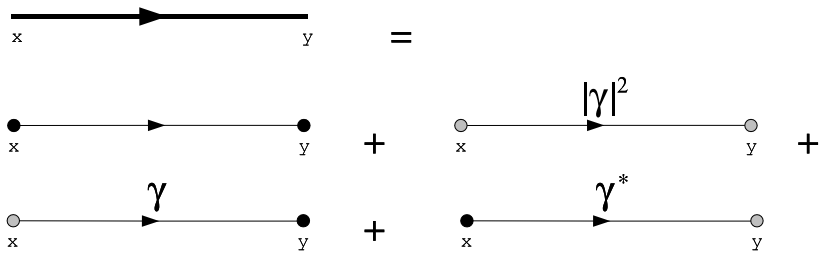

Figure 5.1: Feynman diagram for (5.11). The thick line represents the α-vacuum propagator $G_\alpha(x,y)$. Thin lines represent Euclidean vacuum propagators with a factor of N_α^2, and the other factors are shown explicitly. Grey dots denote points that appear in propagators as antipodes. We have defined $\gamma = e^\alpha$.

Any correlation function of the form (5.8) in the free theory can be found in terms of products of Green's functions by normal-ordering the creation and annihilation operators, and retaining the fully contracted terms. For example,

$$\begin{aligned} &\langle\alpha|\phi(x)\phi(y)\phi(z)\phi(w)|\alpha\rangle \\ &= G_\alpha(x,y)G_\alpha(z,w) + G_\alpha(x,z)G_\alpha(y,w) + G_\alpha(x,w)G_\alpha(y,z) \end{aligned} \tag{5.14}$$

where we have in mind using (5.11) to expand in terms of the Euclidean vacuum Green's functions. Note it is important the ordering of the arguments of the Green's functions is inherited from the ordering in the operator expression on the left-hand side. This is because we are stating the generalized Wick's theorem in the form of Wightman functions rather

than the usual form with time-ordered Green's functions [98]. The expansion of operator products in free field theory using Wightman functions actually predates Wick's theorem [65]. The theorem may be extended to time-ordered expectation values by replacing the Wightman functions with time-ordered two-point functions.

To convert some diagram written in terms of the G_α's into one in terms of Euclidean propagators, replace each thick line with a sum of 4 thin ones. To find the coefficient of each term just count up the number of grey dots, noting their orientation with respect to the arrows. This is written more compactly using the two index notation (5.12), with an index $i = 0, 1$ appearing at the end of each propagator, and all indices summed over.

5.2 Interacting fields

So far all we have said is valid regardless of whether we work on de Sitter space, or its Euclidean continuation, the four-sphere. Once we introduce interactions, however, the choice of Lorentzian versus Euclidean signature has a major impact on the formalism used to setup the perturbative expansion. This is familiar from finite temperature field theory where one has an imaginary time formalism [2, 69] or alternatively one can use a formulation in terms of real time propagators at the price of doubling the number of fields [94, 73].

Describing interacting fields in curved spacetime with event horizons using Lorentzian signature formalism is problematic. Inevitably one must deal with propagators on opposite sides of the horizon, and this leads to ambiguities in the formulation of Feynman rules. The same problem exists for spacetimes with cosmological horizons, as would arise if one attempted to quantize a field in de Sitter space in the static coordinate patch. To avoid

these issues we formulate interacting field theory using the imaginary time, or Euclidean continuation, as advocated in [60]. Eventually we have in mind defining real-time ordered correlators which may be used to construct in-out S-matrix elements as described in [36, 19].

In the Euclidean vacuum, this problem has been much studied in the literature [3, 4, 38, 40, 39, 41] and corresponds to doing field theory on S^4. Our strategy will be to use (5.6) to define the interacting α-vacuum, and construct physical observables as correlators of the field ϕ which couple locally to physical sources. To evaluate these observables we set up the perturbation theory on the Euclidean sphere as a non-local field theory in terms of $\tilde{\phi} = \mathscr{U}^\dagger \phi(x) \mathscr{U}$. We define these fields as interaction picture fields, and will work with the standard methods of canonical quantization.

The interacting part of the non-local action for $\tilde{\phi}$ is obtained by conjugating the local bare interaction terms written in terms of the ϕ fields with the operator U, or more precisely

$$T_\tau e^{iS^{int}_{non-local}(\tilde{\phi})} \equiv \mathscr{U}^\dagger T_\tau e^{iS^{int}_{local}(\phi)} \mathscr{U} \tag{5.15}$$

where T_τ denotes imaginary time ordering. The actions are obtained by integrating the lagrangian density describing the interactions (which we assume to be polynomial in ϕ) over the Euclidean sphere. We note that when (5.9) is substituted into this expression, the anti-podal components $\phi_1(x)$ are to be ordered according to x rather than $\bar{x}$, since the ordering is to be inherited from the right-hand side of (5.15). The determination of any correlation function of ϕ's in an α-vacuum then reduces to a standard Euclidean vacuum correlator computation, albeit with some terms involving fields with unconventional time

ordering. That is, we expand (5.15) perturbatively in the interactions, generating a sum of correlators of $\tilde{\phi}$ with respect to the Euclidean vacuum. These may then be evaluated using the generalized Wick's theorem of the previous section.

Working on the Euclidean sphere has the advantage that a wide range of sensible cutoffs are available. For example one can choose dimensional regularization as in [38,40,39,41], or simply a mode cutoff corresponding to a cutoff on angular momentum on the 4-sphere. Pauli-Villars is another option, as is point-splitting (with spherically symmetric averaging assumed to restore the symmetries), or zeta-function regularization [19, 26, 37]. Little of what we say in the present work is dependent on a particular choice of cut-off.

Let us comment further on the form of the correlators. The normalized Green functions in the α-vacuum take the form

$$\begin{aligned} G(x_1,\cdots,x_n) &= \frac{\langle \mathscr{U}^\dagger T_\tau \phi(x_1)\cdots\phi(x_n) e^{iS^{int}_{local}(\phi)}\mathscr{U}\rangle}{\langle \mathscr{U}^\dagger T_\tau e^{iS^{int}_{local}(\phi)}\mathscr{U}\rangle} \\ &= \frac{\langle T_\tau \tilde{\phi}(x_1)\cdots\tilde{\phi}(x_n) e^{iS^{int}_{non-local}(\tilde{\phi})}\rangle}{\langle T_\tau e^{iS^{int}_{non-local}(\tilde{\phi})}\rangle}. \end{aligned} \tag{5.16}$$

In imaginary time we cannot take an asymptotic limit where interactions turn off, which is important in the usual definition of the S-matrix to obtain the interacting vacuum. Instead we will simply compute correlators with respect to the free vacuum as in (5.16). As usual the denominator in (5.16) implies we drop disconnected diagrams when we compute Green functions. [1] Because we are not taking an LSZ type limit, the relevant Green functions correspond to unamputated diagrams. We discuss continuation to real-time amplitudes in the next section.

[1] By *disconnected* we mean diagrams not connected to external lines.

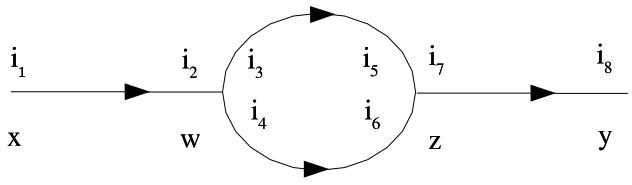

Figure 5.2: Feynman diagram for propagator in $\lambda\phi^3$. The indices i_k label end-points of the propagators G_{ij}. All indices are to be summed over. Vertex factors carry no i_k dependence.

Let us now go through an example to illustrate the renormalization of mass in $\lambda\phi^3$. The relevant Feynman diagram in position space is shown in (5.2). The vertex $V_{ijk} = 1$ for all i, j, k, so the amplitude is

$$A = \sum_{\{i_k=0,1\}} \int \sqrt{\det g_{\mu\nu}(w)}dw\sqrt{\det g_{\mu\nu}(z)}dz G^F_{i_1 i_2}(x,w)G^F_{i_3 i_4}(w,z)G^F_{i_5,i_6}(w,z)G^F_{i_7 i_8}(z,y) \tag{5.17}$$

where G^F is the time-ordered Green function

$$G^F(x,y) = \theta(x^0 - y^0)G_\alpha(x,y) + \theta(y^0 - x^0)G_\alpha(y,x)\ , \tag{5.18}$$

and x^0 is the imaginary time coordinate on the sphere. UV divergences arise when $w \to z$ or $w \to \bar{z}$. In these limits the propagator has the form

$$\lim_{w\to z} G^F(w,z) = N_\alpha^2(1+|\gamma|^2)\frac{1}{(w-z)^2}\ , \qquad \lim_{w\to \bar{z}} G^F(w,z) = N_\alpha^2(\gamma+\gamma^*)\frac{1}{(w-\bar{z})^2} \tag{5.19}$$

in locally Minkowski coordinates. The UV divergent part of the amplitude is then

$$A_{UV} = \frac{\delta m^2}{2} \int \sqrt{\det g_{\mu\nu}(z)} dz \langle \mathscr{U}^\dagger \phi(x) \phi(z)^2 \phi(y) \mathscr{U} \rangle \tag{5.20}$$

where δm^2 is the cutoff dependent counter-term. If we adopt a simple point-splitting regularization, this is given by

$$\begin{aligned} \delta m^2 &= \left(\int_{|w-z|\geq\varepsilon} + \int_{|w-\bar{z}|\geq\varepsilon} \right) \sqrt{\det g_{\mu\nu}(w)} dw \sum_{i_k} G_{i_3 i_4}(w,z) G_{i_5 i_6}(w,z) \\ &\propto N_\alpha^4 \left((1+|\gamma|^2)^2 + (\gamma+\gamma^*)^2 \right) \log \varepsilon \, . \end{aligned} \tag{5.21}$$

We conclude therefore that the counter-term is indeed simply a local mass counter-term when expressed in terms of ϕ variables, but appears non-local when written in terms of $\tilde{\phi}$ variables.

It is perhaps worthwhile to highlight the difference between our computation and a similar computation of [12]. Reference [12] assumed the basic vertex was local. However in our formulation of the α-vacuum field theory, the vertex takes the form $\mathscr{U}^\dagger \phi(z)^3 \mathscr{U}$ which looks non-local when we expand this out in terms of the fields $\phi_0(z)$ and $\phi_1(z)$, since we can view ϕ_1 as localized at $\bar{z}$. This non-locality is exactly what we need to make sense of the non-local counter-terms encountered in [12]. When all the diagrams are included the coefficients of the non-local counter-terms are such that they arise from the local counter-term $\frac{1}{2}\delta m^2 \phi(x)^2$, prior to conjugation by the $\mathscr{U}$'s. This implies the α-vacuum perturbation theory is rendered finite by the same number of renormalization conditions as the corresponding Euclidean vacuum theory.

5.3 Real-time correlators and causality

We now discuss how to continue the imaginary time Green functions to real time. In general this procedure is rather difficult as the analytic continuation is not uniquely defined. One encounters similar problems in the formulation of Minkowski space quantum field theory at finite temperature [50,49,48,59]. There the analytic continuation from imaginary time to real-time, with the extra condition that propagators be analytic in the lower half frequency plane, computes retarded Green functions. Retarded and advanced Green functions may be further combined to give real time-ordered Green functions. This procedure of determining propagators by analytic continuation can be avoided by working with the real-time thermo-field expansion of [94], where the field content is doubled. In thermo-field theory, one also can formulate a non-perturbative path integral definition of the theory using a non-trivial real-time integration contour. It would be interesting to see if the α-vacuum theory could be formulated in an analogous way. We will not develop that here, but content ourselves for the moment with the perturbative description of the theory described in the previous section. We will use these results to obtain the analytic continuation to real-time of the general interacting two-point function.

The general two-point function G in the interacting theory is

$$G(x,y) = \langle \Omega | \phi(x)\phi(y) | \Omega \rangle \tag{5.22}$$

and is perturbatively defined by (5.16). We use $\phi(x)$ to denote Heisenberg operators in this

section. We can insert a complete set of states to obtain

$$G(x,y) = \sum_{\chi,n} \langle \Omega | \phi(x) | \chi, n \rangle \langle \chi, n | \phi(y) | \Omega \rangle \tag{5.23}$$

where $|\chi, n\rangle$ denotes a scalar state with quantum numbers n. We now use de Sitter symmetry to translate $\phi(x) = T\phi(0)T^{-1}$, where T is a de Sitter translation. $|\Omega\rangle$ is invariant under this translation. Usually one would assume $T^{-1}|\chi, n\rangle = \phi_n^E(x)|\chi\rangle$, but as we have learnt, invariance under the subgroup of the de Sitter group continuously connected to the identity, in general only implies $T^{-1}|\chi, n\rangle = N_{\alpha(\chi)}(\phi_n^E(x) + e^{\alpha(\chi)}\phi_n^{E*}(x))|\chi\rangle$, where α is now a function of the state χ, and $\phi_n(x)$ is the generalization of the modes to a scalar field of general mass $m(\chi)$. This implies

$$G(x,y) = \sum_{\chi} \rho(\chi) G_{\alpha(\chi)}(m(\chi); x, y) \tag{5.24}$$

where ρ is positive semi-definite. We can choose to parameterize this instead as

$$G(x,y) = \int_{m_{min}}^{\infty} dm \int d\alpha d\alpha^* \rho(m,\alpha) G_\alpha(m; x, y) \tag{5.25}$$

where $G_\alpha(m; x, y)$ is the generalization of (5.13) to a free field of mass m. In [25] it was argued $m_{min} = 3/2$ for the theory in the Euclidean vacuum. The $m > 3/2$ scalar representations of the de Sitter group are known as the principal series, and only these have a smooth limit to representations of the Poincare group as $H \to 0$ [52]. The $0 < m < 3/2$ representations are known as the complementary series. There do not appear to be any obvious problems with quantizing fields with $0 < m < 3/2$. For example, the conformally coupled

free scalar ($m = \sqrt{2}$), is related by a conformal transformation to a massless field in flat space. Since we are often interested in fields with $m < 3/2$, we include the complementary series in our space of allowed states, so take $m_{min} = 0$.

The $i\varepsilon$ prescriptions for the propagators G_{jk} are defined in appendix B, which allows the G to be continued to a function regular on the Lorentzian section. This prescription is fixed by imposing the boundary condition that each component of the two-point function $G_\alpha(m;x,y)$ match the free Wightman propagators constructed by Mottola and Allen [78,6]. Appropriate linear combinations of $G(x,y)$ define the real-time retarded, advanced, and time-order propagators. We note the complete propagator G is not analytic in the lower half t plane (see appendix B for notation), but it is built out of terms, each of which separately enjoys analyticity in the upper or lower half t plane.

Demonstrating causality of the interacting two-point function is now trivial. We simply apply (5.25) to the commutator of two fields

$$\begin{aligned} \langle[\phi(x),\phi(y)]\rangle_\alpha &= G(x,y) - G(y,x) \\ &= \int_0^\infty dm d\alpha d\alpha^* \, \rho(m,\alpha)(G_\alpha(m;x,y) - G_\alpha(m;y,x)) \\ &= \int_0^\infty dm d\alpha d\alpha^* \, \rho(m,\alpha)(G_E(m;x,y) - G_E(m;y,x)) \end{aligned} \tag{5.26}$$

which vanishes at spacelike separations of x and y. Here we have used the result of [6] that the commutator in the free theory is independent of α.

To sum up, we have defined a continuation of the general interacting two-point function from imaginary time to real time, using a spectral theorem and we have shown the real-time commutator function is causal despite the apparent non-analyticity of the perturbative

expansion.

5.4 Stress-Energy Tensor

Numerous techniques for calculating $\langle T_{\mu\nu} \rangle$ in general, and in the Euclidean vacuum of de Sitter space in particular, are reviewed in [19, 26, 37] and references therein. Since [16] considered the stress-energy tensor in the α-vacua some time ago, we mainly quote their results. The stress-energy tensor for a scalar field is given by

$$T_{\mu\nu} = \phi_{,\mu}\phi_{,\nu} - \tfrac{1}{2} g_{\mu\nu} \phi^{,\alpha} \phi_{,\alpha} + g_{\mu\nu} V(\phi) \tag{5.27}$$

where, for simplicity, we have set the $R\phi^2$ coupling to 0.

In general, we can find the renormalized expectation value of $T_{\mu\nu}$ for a non-interacting scalar field from the symmetric Greens function $G^{(1)}_{xy} = \langle \{\phi_x, \phi_y\} \rangle$, as follows:

$$\begin{aligned} &\langle T_{\mu\nu}(x) \rangle^{free}_{ren} = \\ &\lim_{x',x'' \to x} \left(\nabla_{\mu'} \nabla_{\nu''} - \tfrac{1}{2} g_{\mu\nu} \nabla^{\gamma} \nabla_{\gamma''} + \tfrac{1}{2} m^2 g_{\mu\nu} \right) \tfrac{1}{2} \left(G^{(1)}(x',x'') - G_{ref}(x',x'') \right) \end{aligned} \tag{5.28}$$

where G_{ref} is a reference two-point function which removes the singularities in $G^{(1)}$. Note the limit, and G_{ref} must be chosen to preserve covariance and $T^{\mu\nu}{}_{;\nu} = 0$.

Consistent with previous work cited above [16] found for a non-interacting Euclidean

vacuum [26],

$$\begin{aligned}&\langle T_{\mu\nu}\rangle_{ren}^{free} = \\ &-\tfrac{g_{\mu\nu}}{64\pi^2}\Big(m^2(m^2-2H^2)\left(\psi\left(\tfrac{3}{2}-i\nu\right)+\psi\left(\tfrac{3}{2}+i\nu\right)+\ln\left(\tfrac{H^2}{\mu^2}\right)\right) \\ &+\tfrac{8}{3}m^2H^2-\tfrac{359}{180}H^4\Big)\end{aligned} \tag{5.29}$$

where H is Hubble's constant, $\nu = \sqrt{m^2/H^2 - 9/4}$ and μ is some mass renormalization scale. $\langle T_{\mu\nu}\rangle$ for a general α-vacuum, with a non-interacting scalar field, has been found by by [16] to be

$$\begin{aligned}&\langle T_{\mu\nu}\rangle_{ren}^{free} = \\ &-\tfrac{g_{\mu\nu}}{64\pi^2}\tfrac{1+|\gamma|^2}{1-|\gamma|^2}\times \\ &\Big(m^2(m^2-2H^2)\left(\psi\left(\tfrac{3}{2}-i\nu\right)+\psi\left(\tfrac{3}{2}+i\nu\right)+\ln\left(\tfrac{H^2}{\mu^2}\right)+\tfrac{\pi}{\cosh\pi\nu}\tfrac{\gamma+\gamma^*}{1+|\gamma|^2}\right) \\ &+\tfrac{8}{3}m^2H^2-\tfrac{359}{180}H^4\Big)\ .\end{aligned} \tag{5.30}$$

The main difference between (5.29) and (5.30) is an extra factor of $\frac{1+|\gamma|^2}{1-|\gamma|^2}$. The origin of this constant can be seen from the short distance limit of (5.11) which gives $G_\alpha(x,x) \sim \frac{1+|\gamma|^2}{1-|\gamma|^2}G_E(x,x)$. The α-dependence of the short distance singularity means that our counter terms must be α-dependent. The fact that α-dependent counter-terms are required for a finite $\langle T_{\mu\nu}\rangle$ was viewed as problematic in [67]. As we have already emphasized previously these are precisely the sort of counter-terms we naturally expect. We emphasize both (5.29) and (5.30) are proportional to $g_{\mu\nu}$ which is covariantly constant, implying conservation of energy.

An important conclusion we draw from (5.30) is that no imaginary part appears in $T_{\mu\nu}$

(and hence the action at one-loop order). This indicates the α-vacuum is stable at this order. We discuss the possibility of higher order instabilities in the conclusions.

Now to calculate the $\langle T_{\mu\nu}(x)\rangle$ for the interacting case we need to replace the free Green function with the interacting one (and add in $\langle V_I(\phi)\rangle$). The spectral representation (5.25) then yields a straightforward generalization of (5.30).

Chapter 6

Interacting quantum field theory and alpha vacua II

6.1 Introduction

There has been much recent debate about whether quantum field theory in de Sitter space has a unique vacuum invariant under all the continuously connected symmetries of the space. The resolution of this question is crucial to the understanding of possible trans-Planckian effects on the predictions of inflation [76], and observable effects today such as ultra high energy cosmic ray production [91, 5]. These questions are all the more pressing given recent experimental results confirming general predictions of inflation for the cosmic microwave background [82], and of supernova observations consistent with a positive cosmological constant today [83].

At the level of free field theory, de Sitter space has a one-complex parameter family of vacua, dubbed the α-vacua [30,93,78,6]. It was been argued cutoff versions of these can be

relevant during inflation, where α parameterizes the effects of trans-Planckian physics [42, 44, 43, 34, 33]. Others have argued the α-vacua suffer from inconsistencies [67, 45, 12, 31] once interactions are included, and that the Bunch-Davies/Euclidean vacuum state is the unique consistent state.

In this chapter, based on [56], we review existing approaches to this issue, and elaborate on the connections between them. The most straightforward approach, where one treats the vacuum state as a squeezed state fails due to the appearance of pinch singularities, which renders the perturbation theory ill-defined [45]. We emphasize this is not a problem with the ultra-violet structure of the theory, but rather Feynman integrals become ill-defined when propagators on internal lines are null separated.

A potentially more promising approach based on an imaginary time formulation [55] leads to a sensible perturbation theory, and propagators that agree with the imaginary time continuations of the free propagators of [78, 6]. This perturbative expansion can be continued to real-time and written in terms of a path integral with a non-local kinetic term, but local potential and source terms. For the pure scalar field theory, the algebra of observables built out of local products of the fields remains local. However once the theory is coupled to gravity the acausality becomes unavoidable and presumably renders the theory ill-defined, in keeping with the chronology protection conjecture [62].

6.2 Free propagator

6.2.1 Real-time ordering

Having discussed the Wightman functions previously, we now need to discuss more carefully time-ordering prescriptions. Following [6] we define the signed geodesic distance between points as

$$\tilde{d}(x,y) = \arccos \tilde{Z}(x,y)$$

where

$$\tilde{Z}(x,y) = \begin{cases} \eta_{ab} X^a(x) X^b(y) + i\varepsilon, & \text{if } x \text{ to the future of } y \\ \eta_{ab} X^a(x) X^b(y) - i\varepsilon, & \text{if } x \text{ to the past of } y. \end{cases}$$

With this definition $\tilde{d}(x,y) = -\tilde{d}(\bar{x},\bar{y})$. Not that although only points with $Z \geq -1$ are connected by geodesics, $\tilde{d}(x,y)$ can be defined by analytic continuation for $Z < -1$.

The Euclidean vacuum Wightman function is given by

$$G^E(x,y) = c\ {}_2F_1(h_+, h_-; 2; \frac{1+\tilde{Z}}{2}) \tag{6.1}$$

where

$$h_\pm \equiv \frac{3}{2} \pm i\mu, \qquad \mu \equiv \sqrt{m^2 - \left(\frac{3H}{2}\right)^2}, \qquad c \equiv \frac{\Gamma(h_+)\Gamma(h_-)}{(4\pi)^2}$$

This is similar to the previously discussed symmetric Green's functions 6.3.3. Unless otherwise stated, we consider the case $m > 3/2$ in this chapter. Some of the properties of this

function are as follows:

- ❖ a pole when points coincide ($\tilde{Z}=1$)
- ❖ a branch cut running along $\tilde{Z}=(1,\infty)$, where the imaginary part changes sign
- ❖ and asymptotically as $\left|\tilde{Z}\right|\to\infty$

$$G^E(x,y)\propto\left(-\tilde{Z}\right)^{-h_+}\frac{\Gamma(h_--h_+)}{\Gamma(h_-)\Gamma(h_--1)}+\left(-\tilde{Z}\right)^{-h_-}\frac{\Gamma(h_+-h_-)}{\Gamma(h_+)\Gamma(h_+-1)}\ .$$

Using (3.29) and (6.1), the general α-vacuum Wightman function is then explicitly constructed. Note the general α-vacuum Wightman function has poles both at $\tilde{Z}=1$ and $\tilde{Z}=-1$.

There are a number of options for defining real-time ordering of the two-point functions described above. Conventional definitions [6] correspond to

$$iG_F^E(x,y)=\theta(x^0-y^0)G^E(x,y)+\theta(y^0-x^0)G^E(y,x) \tag{6.2}$$

and

$$iG_F^\alpha(x,y)=\theta(x^0-y^0)G^\alpha(x,y)+\theta(y^0-x^0)G^\alpha(y,x)\ . \tag{6.3}$$

with x^0 a global real-time coordinate. These Green functions satisfy the inhomogeneous Klein-Gordon equation

$$(\Box-m^2)G_F(x,y)=-\frac{\delta^4(x-y)}{\sqrt{-g(x)}},\qquad g(x)=\det g_{\mu\nu}(x)$$

with $g_{\mu\nu}$ the spacetime metric. Note $\delta(x-\bar{y})$ does not appear. The propagator (6.2) can be written as

$$iG_F^E(x,y) = c\ {}_2F_1(h_+,h_-;2;\frac{1+Z'}{2}) \tag{6.4}$$

where Z' is defined with the new $i\varepsilon$ prescription

$$Z'(x,y) = H^2\eta_{ab}X^a(x)X^b(y) + i\varepsilon.$$

However, as discussed in [46] another natural time-ordering in the α-vacuum is obtained by ordering the respective terms of (5.9) according to the arguments of the mode functions, x and $\bar{x}$ (when α is real)

$$\begin{aligned} i\tilde{G}^{\alpha}_{EL}(x,y) \;=\; & N_\alpha^2\Big(\theta(x,y)\left(1+|e^\alpha|^2\right)G^E(x,y)+\theta(y,x)\left(1+|e^\alpha|^2\right)G^E(y,x)+ \\ & 2\theta(\bar{y},x)e^\alpha G^E(\bar{y},x)+2\theta(x,\bar{y})e^{\alpha^*}G^E(x,\bar{y})\Big)\ . \end{aligned} \tag{6.5}$$

Note these Green functions do not satisfy the asymptotic boundary condition (5.7) in the infinite past or future. So contrary to [46] (6.5), do not satisfy the correct boundary conditions for the description of a squeezed state. These propagators satisfy the non-local inhomogeneous Klein-Gordon equation [46]

$$(\Box - m^2)\tilde{G}^{\alpha}_{EL}(x,y) = -N_\alpha^2\left(\left(1+|e^\alpha|^2\right)\frac{\delta^4(x-y)}{\sqrt{-g(x)}}+2e^\alpha\frac{\delta^4(x-\bar{y})}{\sqrt{-g(x)}}\right) \tag{6.6}$$

so are to be interpreted as corresponding to source boundary conditions on a linear combination of podal (y) and anti-podal points ($\bar{y}$).

Another natural time ordering is

$$\begin{aligned} i\tilde{G}_F^{\alpha}(x,y) &= N_\alpha^2 \left(\theta(x,y)\left(1+|e^\alpha|^2\right)G^E(x,y)+\theta(y,x)\left(1+|e^\alpha|^2\right)G^E(y,x)+\right. \\ &\quad \left.\theta(\bar{y},x)\left(e^\alpha+e^{\alpha^*}\right)G^E(\bar{y},x)+\theta(x,\bar{y})\left(e^\alpha+e^{\alpha^*}\right)G^E(x,\bar{y})\right) \\ &= iN_\alpha^2\left(\left(1+|e^\alpha|^2\right)G_F^E(x,y)+\left(e^\alpha+e^{\alpha^*}\right)G_F^E(x,\bar{y})\right) \end{aligned} \tag{6.7}$$

which is obtained by time ordering the arguments of the propagators appearing in (3.29). This agrees with the propagator of [46] when α is real, and generalizes it when α is complex. As we will see, these propagators appear on internal lines, when one analytically continues from the imaginary time formulation of [55] to real-time. This propagator satisfies the inhomogeneous Klein-Gordon equation

$$(\Box - m^2)\tilde{G}_F^{\alpha}(x,y) = -N_\alpha^2\left(\left(1+|e^\alpha|^2\right)\frac{\delta^4(x-y)}{\sqrt{-g(x)}}+\left(e^\alpha+e^{\alpha^*}\right)\frac{\delta^4(x-\bar{y})}{\sqrt{-g(x)}}\right) .$$

This Feynman propagator can be written in terms of hypergeometric functions using (6.4).

6.3 Interacting Theory

6.3.1 Squeezed state approach

The most direct approach to setting up the real-time perturbation theory is to define Green functions using the interaction picture representation

$$G(x_1,\cdots,x_n) = \langle E|U^\dagger\, T\left(\phi(x_1)\cdots\phi(x_n)e^{iS_{int}(\phi)}\right)U|E\rangle \tag{6.8}$$

where S_{int} is the interacting part of the action, and T denotes time-ordering with respect to global time. One can view $U|E\rangle$ as a squeezed state defined in the infinite asymptotic past/future of de Sitter and these Green functions may then be used to extract an S-matrix. This expression may be expanded in powers of the interaction by conventional means, and the end result involves Feynman propagators ordered with respect to the global time coordinate (6.3).

As emphasized in [45], pinch singularities arise in these expressions which render the integrals ill-defined. This may be seen in the following example of a diagram that occurs with a $\lambda\phi^4$ interaction. The lower loop gives rise to the factor

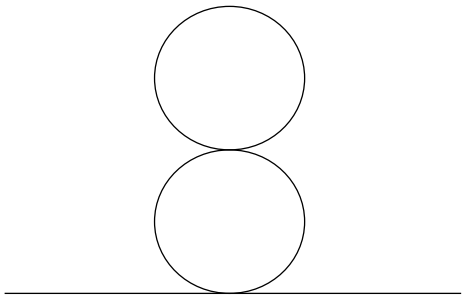

Figure 6.1: Pinch diagram

$$\int_{dS_4} d^4x\sqrt{-g}G_F^{\alpha}(x,y)^2 \tag{6.9}$$

which contains terms like

$$\int_{dS_4} d^4x\sqrt{-g}G_F^{E}(x,y)G_F^{E}(\bar{x},\bar{y}) \ .$$

Writing this in terms of hypergeometric functions (6.1), we see the $i\varepsilon$ prescriptions differ

in the two propagators. The contribution coming from the region of integration where x is null related to y gives a term proportional to

$$\int dZ \frac{1}{Z-1+i\varepsilon}\frac{1}{Z-1-i\varepsilon} = \frac{\pi}{\varepsilon} \tag{6.10}$$

where Z is integrated along the real axis. As $\varepsilon \to 0$ the poles pinch the integration contour and the integral diverges. We emphasize this divergence has nothing to do with the ultraviolet structure of the theory, so cannot be regulated with local (or even bi-local) counter-terms.

This divergence implies that perturbation theory does not make sense as it stands. It is conceivable that some resummation of perturbation theory does make sense, but we lack methods to address this kind of approach in a completely systematic way. We note this type of resummation is attempted in non-equilibrium statistical field theory where one similarly encounters pinch singularities [8, 7]. This resummation can lead to a shifting in the poles of the propagator, so that the $i\varepsilon$ in (6.10) is replaced by an $i\Gamma$ where Γ is a decay rate, proportional to some power of the interactions. It is then clear from (6.10) that the resummed theory will be difficult to handle due to the appear of inverse powers of the coupling.

6.3.2 Imaginary-time approach

Since the direct approach to treating the α-vacua as squeezed states in de Sitter space is a nonstarter, one can try to appeal to an imaginary time formulation [55]. This provides us with a straightforward way to deal with spacetimes with event horizons, since for imaginary time the event horizon shrinks to a point. In the black hole case, field theory on the

imaginary time continuation (also called the Euclidean section) of a black hole background leads to a density matrix description from the real time point of view. One might have hoped a similar novel interpretation of the α-vacua emerges in the real-time point of view, due to the cosmological horizon of de Sitter space.

To discuss the continuation from real time to imaginary time we use global coordinates

$$ds^2 = -d\bar{t}^2 + (\cosh \bar{t})^2 \, d\Omega_3^2$$

so $t \to i\tau$ takes us to imaginary time. Here we have chosen units where $H = 1$. The imaginary time continuation of de Sitter is the four-sphere. The imaginary time approach of [55] proceeds by using the transformation (5.9) to express α-vacuum Green functions as linear combinations of Euclidean vacuum Green functions

$$G(x_1, \cdots, x_n) = \langle E | U^\dagger \phi(x_1) \cdots \phi(x_n) e^{iS_{int}(\phi)} U | E \rangle = \langle E | \widetilde{\phi}(x_1) \cdots \widetilde{\phi}(x_n) e^{iS_{int}(\tilde{\phi})} | E \rangle \ . \quad (6.11)$$

This is to be understood as an interaction picture expression. An important point is that on the Euclidean section, the free propagators $G^\alpha(x,y)$ are symmetric functions of their arguments because points are spacelike separated. The ordering of operators in this expression is therefore irrelevant. As described in [55] the ultraviolet divergences that appear in this approach can be canceled by w Sitter invariant local counter-terms. This approach yields free two-point functions that match those of Mottola and Allen on the Euclidean section, and it is in this sense the approach is a generalization of the α-vacuum to the interacting case. However the real-time physics of this approach is so far mysterious, and we wish to

explore this question in the following.

6.3.3 Continuation to real time

Let us examine what happens when we continue integrals of products of $G^{\alpha}(x,y)$ on the sphere to integrals over de Sitter space. We are free to expand (6.11) as in (3.29) and order the arguments in any way convenient for analytically continuing to real-time. Let us first focus on the case of the Euclidean vacuum $e^{\alpha} = 0$. We begin with the imaginary time contour as shown in figure 6.3.3 running from $-i\pi$ to $i\pi$. This may be continued to the contour shown in figure 6.3.3. The horizontal component (with a small positive slope) running from $-\infty$ to ∞ through points x_1 to x_4 gives rise to the expected real-time contour. The corresponding $i\varepsilon$ prescription is $t \rightarrow t + i\varepsilon$ sgn t which gives a Feynman propagator connecting internal lines (6.4). The vertical components of the contour are closely analogous to those that appear in the real-time formulation of finite temperature field theory in flat space [73, 80]. There the vertical components of the contour typically factorize for Green functions evaluated at finite values of the time. However this factorization is quite subtle [47] even for flat space, so we will not assume it here in general.

The other horizontal components to the time-contour correspond to the fact that one is not computing a transition amplitude, but rather the expectation value of some time-ordered string of field operators with respect to a density matrix specified at some specific time t_0 (where $t_0 = 0$ in figure 6.3.3)

$$G(x_1, \cdots, x_n) = \mathrm{Tr}\rho(t_0) T\left(\phi(x_1) \cdots \phi(x_n)\right) \ . \tag{6.12}$$

The additional time contour represents the time-evolution back to the initial time, as is easy to see when (6.12) is written in Schroedinger picture. The density matrix formalism is discussed in the general context of Friedman-Robertson-Walker backgrounds in [84]. In this work a deformation of the contour shown in figure 6.3.3 is used that only contains two horizontal real-time components (and a single vertical component).

In [31] the same two-component time-contour is used (neglecting the vertical components of the contour), which can be re-expressed in terms of a two-component field formalism. However they use a time-ordering prescription analogous to (6.3), which as we will see is not obtained via analytic continuation of the imaginary time approach. Their main claim was that there exist ultra-violet divergences that cannot be canceled with de Sitter invariant counter-terms. They approximated the α-vacuum by starting with the free field theory state, and then turned on interactions at a finite time. Given that their boundary conditions did not respect de Sitter invariance, the appearance of de Sitter non-invariant counter-terms should not be too surprising. Such features cannot arise in a manifestly de Sitter invariant formulation, so are more properly regarded as renormalization effects associated with the symmetry breaking initial state.

It is natural to conjecture that in-out transition amplitudes relating the vacuum in the infinite past to vacuum in the infinite future, may be computed by including only the horizontal component of the contour running along the real time axis (with small positive slope) as shown in figure 6.3.3. This allows us to express the real-time physics using a single component field. This fits nicely with the expectation that pure states do not evolve into mixed states in a fixed de Sitter background, since the spacetime is globally hyperbolic [1].

[1] In general, when continuing from imaginary-time Green functions to real-time Green functions, pure

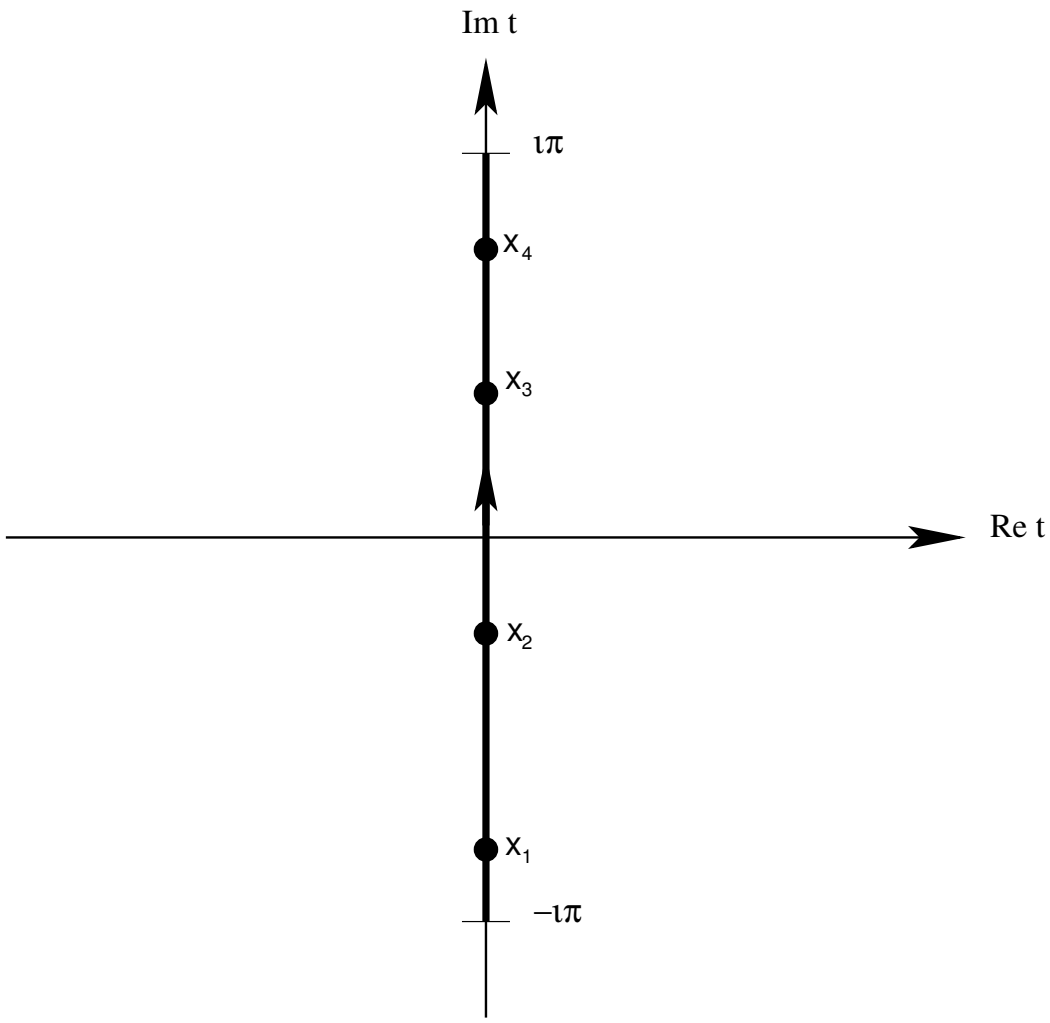

Figure 6.2: Imaginary time contour.

states evolve to mixed states [61].

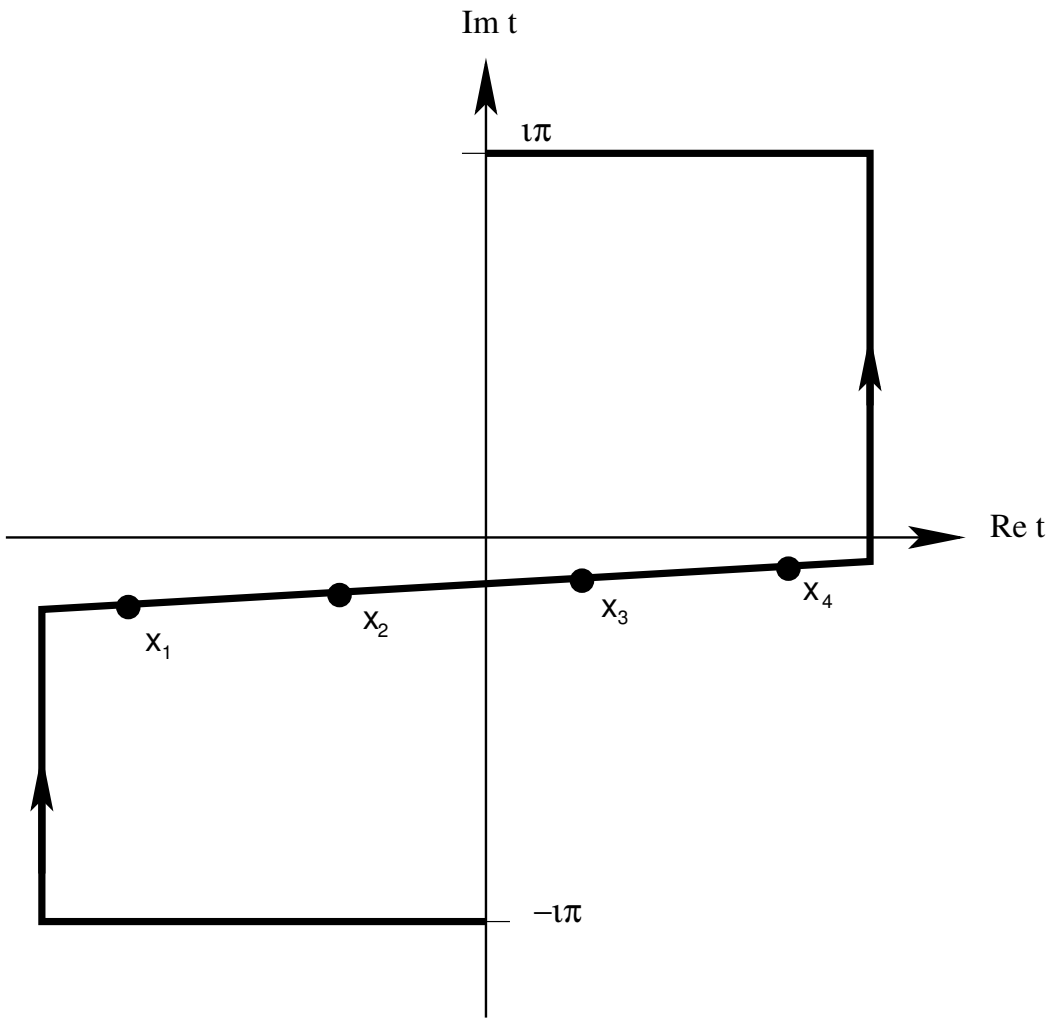

Figure 6.3: Real-time contour. The horizontal components of contours are to be understood to run off to $t = \pm\infty$.

Now let us examine what happens when $e^{\alpha} \neq 0$. Again we start with the imaginary time contour, with a product of imaginary time propagators (3.29). These may be decomposed into Euclidean vacuum correlators as in the second line of (3.29). To continue to real-time, we continue to the contour shown in figure 6.3.3. The real-time continuation of the imaginary time formalism [55] therefore yields a set of amplitudes of the form (6.12), with ϕ's replaced by $\tilde{\phi}$'s.

If we wish to compute only in-out matrix elements, then we retain only the horizontal contour running along the real axis, and we find podal and anti-podal points are to be ordered according to their global time t [46]. Thus the propagators (6.7) will appear on internal lines in the general α-vacuum expression for real-time ordered Green functions. Because all singularities appearing in the propagator have the same $i\varepsilon$ prescription, the resulting integrals are integrals of analytic functions, and no pinch singularities arise. Likewise, no pinch singularities will arise if we use the full contour to compute the continuation of the amplitudes of [55] , though one must then use a multi-component field formalism analogous to [84] to directly perform the real-time computations.

One might wonder whether the single horizontal component plus the vertical components of the contour might lead one back to the in-out amplitudes of the squeezed state approach. This cannot be the case, because the vertical components will not generate pinch singularities, nor will the vertical components change the boundary conditions on the free propagators from (6.3) to (6.7).

6.3.4 Path Integral Formulation

The real-time continuation of the imaginary time formalism just described yields a set of finite renormalized in-out amplitudes of the form

$$G(x_1,\cdots,x_n)=\langle E|T\left(U^{\dagger}\phi(x_1)\cdots\phi(x_n)e^{iS_{int}(\phi)}U\right)|E\rangle=\langle E|T\left(\widetilde{\phi}(x_1)\cdots\widetilde{\phi}(x_n)e^{iS_{int}(\tilde{\phi})}\right)|E\rangle \tag{6.13}$$

where the time-ordering prescription is as in (6.7). Note that by definition local sources couple to the $\tilde{\phi}$ [55], which is a linear combination of the field at podal and anti-podal

points as in (5.9). We will work under the hypothesis that the set of amplitudes (6.13) define a consistent set of probability amplitudes. For example, these could be used to approximate transition amplitudes corresponding to observations of a comoving observer. The general set of local observables should correspond to Wightman functions of the $\tilde{\phi}$.

The time-ordered correlators (6.13) can be generated from the following path integral

$$Z = \int \mathscr{D}\tilde{\phi} e^{iS[\tilde{\phi}]} \tilde{\phi}(x_1) \cdots \tilde{\phi}(x_n)$$

where the action S is

$$S = \frac{1}{2} \int d^4x \sqrt{-g(x)}\, d^4y \sqrt{-g(y)} \tilde{\phi}(x) K(x,y) \tilde{\phi}(y) - \int d^4x \sqrt{-g(x)} \left(V(\tilde{\phi}) + j(x)\tilde{\phi}(x) \right) \tag{6.14}$$

with the non-local kinetic term determined by

$$\begin{aligned} K(x,y) &= \left(a \frac{\delta^4(x-y)}{\sqrt{-g(x)}} + b \frac{\delta^4(x-\bar{y})}{\sqrt{-g(x)}} \right) \left(\Box_x - m^2 \right) \\ a &= \frac{1-|e^{\alpha}|^4}{(1-e^{2\alpha})(1-e^{2\alpha^*})} \\ b &= -\frac{(e^{\alpha}+e^{\alpha^*})(1-|e^{\alpha}|^2)}{(1-e^{2\alpha})(1-e^{2\alpha^*})} \,. \end{aligned} \tag{6.15}$$

This kernel is the inverse of the Feynman propagator (6.7)

$$\int d^4z \sqrt{-g(z)} K(x,z) \tilde{G}_F^{\alpha}(z,y) = -\frac{\delta^4(x-y)}{\sqrt{-g(x)}} \,.$$

It is possible to make a field redefinition to write the kinetic term in local form, but then the

potential term becomes non-local. It is also worth noting that the amplitudes (6.13) cannot be interpreted simply as amplitudes in a squeezed state background, contrary to [46]. This would require the U operators to be commuted past the time-ordering symbol, so that one could define an asymptotic state $U|E\rangle$ in the infinite past. However this step cannot be made due to the non-locality of the theory, as one can easily check using the explicit mode expansions of the amplitudes. Summing up, this approach differs from the squeezed state approach described in section 6.3.1, due to the different time-ordering prescription, which in turn leads to a different non-local kinetic term.

6.3.5 Algebra of observables

Local sources couple directly to $\tilde{\phi}$ and likewise interactions are local (6.14) [55]. If we are interested in the scalar field theory with possible local scalar couplings of other fields to $\tilde{\phi}$, then the set of observables will be built out of local products of $\tilde{\phi}$ and derivatives. As shown in [6], the commutator algebra of the $\tilde{\phi}$ is actually independent of α, and so vanishes at spacelike separations. The same will therefore be true of local products of the $\tilde{\phi}$. Apparently then the pure scalar field theory can give rise to a self-consistent set of probability amplitudes in this approach, which does not allow faster than light signaling. This provides us with a posteriori justification for taking the single-component real-time contour leading to (6.13).

However gravity couples locally to the stress-energy tensor

$$\begin{aligned} T_{\mu\nu}(x) &= \frac{2}{\sqrt{-g(x)}}\frac{\delta S[\tilde{\phi}]}{\delta g^{\mu\nu}(x)} \\ &= a\left(\tilde{\phi}_{;\mu}(x)\tilde{\phi}_{;\nu}(x) - \tfrac{1}{2}g_{\mu\nu}(x)g^{\rho\sigma}(x)\tilde{\phi}_{;\rho}(x)\tilde{\phi}_{;\sigma}(x) + \right. \\ &\quad \left.\tfrac{1}{2}m^2\left(\tilde{\phi}(x)\right)^2 g_{\mu\nu}(x)\right) + \\ &\quad \left(V(\tilde{\phi}(x)) + j(x)\tilde{\phi}(x)\right)g_{\mu\nu}(x) + \\ &\quad b\left(\tfrac{1}{2}\tilde{\phi}_{;\mu}(x)\tilde{\phi}_{;\nu}(\bar{x}) + \tfrac{1}{2}\tilde{\phi}_{;\mu}(\bar{x})\tilde{\phi}_{;\nu}(x)\right. \\ &\quad \left.-\tfrac{1}{2}g_{\mu\nu}(x)g^{\rho\sigma}(x)\tilde{\phi}_{;\rho}(x)\tilde{\phi}_{;\sigma}(\bar{x}) + \tfrac{1}{2}g_{\mu\nu}(x)m^2\tilde{\phi}(x)\tilde{\phi}(\bar{x})\right) \end{aligned}$$

which is non-local in the $\tilde{\phi}$'s due to the non-local kinetic term (6.15). The commutator of $T^{\mu\nu}$ with a local product of $\tilde{\phi}$ can therefore be non-vanishing at spacelike separations. Therefore once the scalar field is coupled to gravity, the locality of the observables is spoiled and faster than light signaling becomes possible. This should be taken as a sign that the theory is non-perturbatively ill-defined once coupled to gravity. Once faster than light signaling is possible, it should be possible to consider processes analogous to closed timelike curves, which typically lead to uncontrollable quantum backreaction [62]. We emphasize this is not acausality at Planck scale separations, but macroscopic acausality induced by propagation of the massless graviton. Even if these terms appear with tiny coefficients (as they would based on the arguments of [54, 5]), there is no known theoretical framework for handling such processes.

One could try to fix this problem by placing the graviton itself in an α-state, by instead demanding a linear combination of $g_{\mu\nu}(x)$ and $g_{\mu\nu}(\bar{x})$ couple locally to $T^{\mu\nu}$. As with the

$\tilde{\phi}$ field, the new graviton will then have a non-local kinetic term. This may well work at the linearized level around a fixed de Sitter background, but once we include gravitational interactions and proceed to write down a diffeomorphism invariant action, one will run into problems. For the pure scalar field theory to work it was important that interactions were local, despite the non-local kinetic term. However, if we start with the non-local gravitational kinetic term and add interactions order by order in Newton's constant to achieve diffeomorphism invariance, we will induce non-local gravitational interaction terms. Again it seems impossible to avoid problems with faster than light signaling.

Furthermore the anti-podal symmetry is a special feature of de Sitter space that will not generalize in a background independent way. One could try to define the theory on the Lorentzian continuation of $\mathbb{RP}^4$, making the identification $x \sim \bar{x}$. Here the gravitational action takes the conventional Einstein-Hilbert form, but it is not clear how to make sense of physics on such a spacetime. One could take as a fundamental region the inflationary patch

$$ds^2 = 1/\grave{\eta}^2 \left(-d\grave{\eta}^2 + d\vec{x}^2\right) ,$$

and treat $\grave{\eta}$ as the global time coordinate. However, we saw in 2.6 that the spacetime is not time orientable. As described in [81], this implies global quantization of a free scalar field on this spacetime is not possible. In [81] it is argued scalar field quantization within a single static patch can be done self-consistently. However without a global quantization method, one must go well beyond the conventional framework of semi-classical quantum gravity to make sense of the coupling of such a system to gravity. Furthermore, we saw in 2.6 that it is not clear how to make sense of that spacetime as a cosmological background.

For the Bunch-Davies vacuum all these problems are avoided, because the kinetic term is local for $e^{\alpha} = 0$. We conclude that the Bunch-Davies vacuum is the only de Sitter invariant vacuum state that yields a consistent conventional perturbative quantum field theory when coupled to gravity.

Chapter 7

Ultra-High Energy Cosmic Rays and alpha vacua

7.1 Introduction

In this chapter, based on [5], we discuss how the presence of a cut-off α-vacuum at the present time could produce ultra high energy cosmic rays. Assuming that we are presently asymptoting to a de Sitter phase, it is argued that the observed flux of cosmic rays bounds the value of parameterα. Saturating the bound gives a new mechanism for the top-down production of super-GZK cosmic rays. The scenario is similar to the production of super-GZK cosmic rays by the decay of galactic halo super-heavy dark matter particles. An initial study along these lines was made in [91] where the contribution to the cosmic ray spectrum was considered.

The cosmic ray spectrum has a feature at around 5×10^{18}eV where the power-law spectrum flattens from $E^{-3.2}$ to $E^{-2.8}$ as E increases, which suggests a transition from a

galactic component of conventional astrophysical origin, to a component of extra-galactic origin. Some recent reviews of theoretical and experimental prospects for the study of these ultra high energy cosmic rays may be found in [9,17]. Above about 10^{20}eV, protons rapidly lose energy due to their interaction with the cosmic microwave background, leading to the GZK cutoff [58,99]. A handful of events (~10) above this bound have been observed, and there is still come controversy over whether or not the cutoff has been observed [95,64,1]. Extremely high energy cosmic rays $\gtrsim 10^{20}$eV are difficult to explain using conventional physics because likely sources lie outside the 100 Mpc range of $\gtrsim 10^{20}$eV protons. A wide variety of scenarios have been proposed to account for the super-GZK events, which break down into two main classes: bottom-up mechanisms where charged particles are accelerated in large scale magnetic fields, and top-down mechanisms where exotic particles/topological defects produce extremely high energy cosmic rays via decay.

The α-vacua provide us with a new top-down mechanism for the production of extremely high energy cosmic rays. As noted in [20], a comoving detector can detect transitions of arbitrarily large energies (which we assume are cutoff near the Planck scale). The exception is the Bunch-Davies vacuum, where a detector measures a thermal response with a temperature of order the Hubble scale. These very high energy transitions in a generic α-vacuum can then account for production of extremely high energy cosmic rays.

Starobinsky and Tkachev [91] argued that if the α-vacua do contribute to the ultra high energy cosmic ray spectrum at around 10^{20}eV, then the value of α becomes so tightly constrained that it would not produce observable effects during inflation[1]. In the present

[1] Starobinsky and Tkachev analyze the situation where the vacuum is a mode number independent Bogoliubov transformation relative to the Bunch-Davies vacuum. Although they did not refer to them as such, these are the α-vacuum states studied earlier in [30,93,78,6].

paper, we revisit this question and argue a much weaker constraint on α follows from cosmic ray observations. Our analysis also has bearing on the general question of what a low-energy observer will see in an α-vacua. The upshot of our analysis is that because production of cosmic ray flux necessarily violates de Sitter invariance, the production rate will be proportional to the background number density of matter, which leads to a much suppressed production rate versus the estimates of [91]. This rate is calculated in detail in section 7.2.

From this result we infer bounds on $\alpha$from cosmic ray observations. Assuming these bounds are saturated, we find the α-vacua give predictions very similar to extremely high energy cosmic ray production via decaying super-heavy dark matter in the galactic halo. This scenario has already been much studied in the literature [72, 18, 14]. We check that observable signals are out of reach in current neutrino/proton decay detectors. Finally we argue CPT violation in an α vacuum does not give rise to baryogenesis.

7.2 Comoving Detector in de Sitter Space

In a de Sitter invariant vacuum state, all correlators are invariant under the continuously connected symmetries of de Sitter space. In particular, this implies that $\langle n^\mu \rangle = 0$ for all 4-vectors n^μ, such as the number flux. Equivalently, the stress energy tensor in the de Sitter vacuum is proportional to the metric $T_{\mu\nu} \propto g_{\mu\nu}$. Since the metric is diagonal in comoving coordinates, this implies the absence of fluxes of energy or momentum. However a co-moving detector nevertheless makes transitions due to its passage through the background spacetime, via the Unruh effect. We will model the injection spectrum of ultra high energy

cosmic rays by viewing the universe today as de Sitter with $H = H_0$, the value of the Hubble parameter today. We treat the background density of ordinary Standard model matter as a small perturbation that explicitly breaks the de Sitter symmetry. Under certain circumstances, we can then treat these matter particles as Unruh detectors, which make transitions to highly excited states via interaction with the nontrivial vacuum state.

The α parameter in principle can depend on the species of field [55], which introduces a high degree of model dependence in the predictions. For simplicity let us model the fields of observable matter by a single scalar field χ and assume that a different field ϕ (for example, the inflaton) is in a nontrivial α-vacuum, with coupling $\chi^2\phi$. We assume an order 1 coupling of ϕ to observable Standard model matter fields. The linear coupling of ϕ then allows us to treat the χ particles as an Unruh detectors (see [19] for a review).

As shown in [20] the rate at which an Unruh detector makes transitions is

$$\Gamma = N_\alpha^2 \left|1 + e^{\alpha + \pi\Delta E/H}\right|^2 \Gamma_0 \tag{7.1}$$

where Γ_0 is the result in the standard Bunch-Davies vacuum, $N_\alpha^2 = \frac{1}{1-e^{\alpha+\bar{\alpha}}}$. Γ_0 is Boltzmann suppressed by a $e^{-2\pi\Delta E/H}$ factor, so for large ΔE, Γ is proportional to $N_\alpha^2 |e^\alpha|^2$ times a power of ΔE^2. The injection spectrum is dominated by $\Delta E \sim M_c$ the field theory cutoff scale, which we have in mind to be of order the GUT scale 10^{16}GeV. When we integrate over ΔE, dimensional analysis then implies the total transition rate is

$$\Gamma \approx N_\alpha^2 |e^\alpha|^2 M_c. \tag{7.2}$$

[2] $\Gamma \sim N_\alpha^2 \left|1 + e^{\alpha+\pi\Delta E/H}\right|^2 e^{-2\pi\Delta E/H} \sim N_\alpha^2 \left|e^{-\pi\Delta E/H} + e^\alpha\right|^2 \sim N_\alpha^2 |e^\alpha|^2$

Here we have assumed e^{α} is not so small that the 1 dominates in the $1+e^{\alpha+\pi\Delta E/H}$ factor of (7.1). It is straightforward to generalize this expression to models with different couplings of α-vacuum species to observable matter, using the general formula (7.1).

7.3 Ultra High Energy Cosmic Ray Production

Let us begin by reviewing the α-vacuum scenario, as described in [54]. During inflation, trans-Planckian effects [76] can lead to a de Sitter invariant state that differs from the conventional Bunch-Davies vacuum. If we invoke "locally Lorentzian" boundary conditions on modes, as described in [34, 33], one finds

$$e^{\alpha} \sim H/M_c. \tag{7.3}$$

This modifies inflationary predictions for the cosmic microwave background spectrum [34, 33, 54]. At the end of inflation, the value of the cosmological constant changes drastically. The squeezed state corresponding to the α-vacuum will then generate particles, producing an energy density of order [54, 91]

$$\varepsilon \sim N_{\alpha}^2 |e^{\alpha}|^2 M_c^4. \tag{7.4}$$

Provided $M_c \ll M_{Planck}$ this particle production does not overclose the universe, and instead can be thought of as some component of particle production during reheating. This energy density will decay in a time of order $1/M_c$ (up to coupling dependent factors), as is typical of unstable particle production during reheating.

At much later epochs, it is still possible to have a residual α-vacuum present. If the universe asymptotes to a de Sitter universe with cosmological constant determined by the present value of H, the arguments of [34, 33] again apply and we can expect α given by (7.3) [54, 35]. One can then ask what phenomena observers today will see to indicate the presence of the α-vacuum. In [91] the assumption was made that (7.4) will be present for all times, and they used this to constrain α by matching with observed ultra high energy cosmic ray production. This assumption is equivalent to computing the energy density of the α-vacuum with respect to the Bunch-Davies vacuum, but gives the wrong result if the future asymptotic vacuum state is the α-vacuum. In this case, as we described in section 7.2, no additional particle creation will be present in the de Sitter phase, and instead the particle production will be determined by (7.2), where we treat background matter as individual Unruh detectors.

In reality, the present universe is far from a pure de Sitter phase. The pure de Sitter estimate of the production rate nevertheless should be a reasonable order of magnitude estimate of the present rate of high energy particle production. Of course without a more detailed model for the dynamics that governs α we cannot make more precise statements.

Let us proceed then to compute the rate of high energy particle production in an α-vacuum. By the arguments of section 7.2, we can then treat each Standard model particle as an Unruh detector, so (7.2) gives the rate of production per unit volume as

$$\frac{dn}{dt} = \Gamma n \tag{7.5}$$

where n is the number density of Standard Model particles [3]. In the situation of interest here, this density will be of order the baryon number density n_B which is typically

$$\begin{aligned} n_B &= 10\,\mathrm{m}^{-3} \approx H^2 M_{Planck}^2/m_p \quad \text{critical density} \\ &= 10^6\,\mathrm{m}^{-3} \qquad\qquad\qquad\qquad\quad \text{interstellar space} \end{aligned}$$

where m_p is the proton mass. Plugging in numbers, we find the dominant source of high energy cosmic rays will come from within our own galaxy due to interaction of visible and dark matter with the α vacuum. Many of the predictions will therefore be similar to the class of top-down models for ultra high energy cosmic ray (UHECR) production from decaying super-heavy dark matter particles in the galactic halo. For a galactic halo of size r_{halo} , we find the flux received on earth will be of order

$$j \approx \Gamma n_B r_{halo}.$$

The experimental bounds coming from UHECR production gives $jE^2 \approx 10^{24}$ eV^2 m^{-2} s^{-1}sr^{-1} at $E \approx 10^{20}$ eV. Assuming $r_{halo} \approx 10^5$ light years, this translates into a bound

$$|e^\alpha| \lesssim 10^{-42} \left(\frac{10^{16}\mathrm{GeV}}{M_c}\right)^{1/2}. \tag{7.6}$$

This is to be compared with the "natural value" $e^\alpha \sim H/M_c \approx 10^{-61} M_{Planck}/M_c$ which is much smaller. We conclude then if ultra high energy cosmic ray production is to be accounted for by the α vacuum then the value of α must be much larger than its natural

[3] The earlier calculation of [91] obtained $dn/dt \sim |e^\alpha|^2 H M_c^3$ (converting to our notation). Our result (7.5) is suppressed by a factor of order $HM_{Planck}^2/m_p M_c^2$, where the reader should recall H is the Hubble parameter today, and we have substituted the critical density for n.

value.

It is interesting to ask if such a large value for α today might have other observable consequences. Let us also estimate the time needed for a neutrino style detector to see a nontrivial interaction with the α-vacuum. The interaction rate per baryon is (7.2) (taking $e^{\alpha} = H/M_c$, and $M_c = 10^{16}$GeV)

$$\Gamma = 10^{-76} s^{-1}$$

which is about 36 orders of magnitude smaller than current bounds on proton decay rate. For α saturating the bound (7.6) and $M_c = 10^{16}$GeV, we instead get

$$\Gamma = 10^{-44} s^{-1}$$

which is only 4 orders of magnitude smaller than the bounds on proton decay. We conclude that even if α is so large as to account for UHECR production, other means of direct detection will be difficult.

Finally, one might ask whether the present analysis has some impact on the spectrum of primordial inflation fluctuations. During the inflationary phase, the effect of the α-vacua on the primordial spectrum has been discussed in [34, 33, 54, 43], where it was found the amplitude of the spectrum was modulated by a factor of the form $1 + \mathcal{O}(H/M_c)$. The particle production effects described in the present paper will be absent in empty de Sitter, and we expect the effect will be a small correction to the energy density (7.4) in the context of slow-roll inflation. Note we already constrain (7.4) to be less than the vacuum energy

density during inflation [54]. Therefore we expect the particle production effects described here will have negligible impact on the spectrum of primordial fluctuations.

7.4 Baryogenesis

An interesting feature of the α vacua is that they violate CPT symmetry when α is not a real number [6, 20]. This opens the possibility that the α vacua could be used to explain baryogenesis. If the CPT violation gives rise to particle/anti-particle mass differences, then baryogenesis could occur in thermal equilibrium, and might be relevant during the reheating phase at the end of inflation.

Greenberg [57] has argued that particle/anti-particle mass differences are only possible in flat space, if one gives up locality. We can apply these general results in the short wavelength limit of α vacuum propagators. As shown in [55] the interacting propagators give rise to local commutators in α vacua. In this limit, de Sitter symmetry becomes local Lorentz symmetry, so Greenberg's result will carry over. We conclude that α vacua do not lead to this type of baryogenesis.

Chapter 8

Conclusions

We have constructed a very simple class of initial states for the inflaton field which can be used to model effects of trans-planckian physics. A new cosmological observable emerges from this analysis in the context of slow-roll inflation, namely the α parameter characterizing the vacuum state during inflation.

Other previous approaches have typically assumed some definite model for the trans-planckian physics which led to particular states of this type at momenta much below the Planck scale. We have found for certain ranges of parameters, the initial states do not lead to excess particle production at the end of inflation, and lead to potentially observable corrections to the cosmic microwave background spectrum.

To counter objections to the theoretical consistency of these states, we have constructed a renormalizable perturbation theory for scalar field amplitudes in an α vacuum using an imaginary time formulation. We have also shown the theory is causal when continued to real-time, at the level of the two-point function.

The formalism we have developed may also have useful generalizations to compu-

tations in flat space in squeezed state backgrounds. See [92] for QED calculations in squeezed state backgrounds.

However, we have seen that from the current theoretical standpoint, the α-vacua are in general inconsistent. The most straightforward treatment as a squeezed state leads to pinch singularities which render the perturbative expansion ill-defined. Another approach derived from imaginary time methods leads to a well-defined perturbative expansion, however the theory becomes non-local once coupled to gravity. We stress this non-locality is over macroscopic scales due to the fact it is induced by the massless graviton, so does not have a local effective description even at arbitrarily low energies. Conventional wisdom then suggestions the vacua cannot be consistently coupled to gravity at the non-perturbative level. Hopefully these results serve to pin-point the problems with the so-called α-vacua, and establish the Bunch-Davies vacuum as the unique de Sitter invariant vacuum state that survives coupling to gravity.

These results have a number of important implications for trans-Planckian effects during inflation. Certain classes of trans-Plankian effects can be modelled as an α-vacua with an explicit ultra-violet cutoff as advocated in [54, 34]. In these models it is presumed unknown ultra-violet physics place modes in an α-vacuum below some proper cutoff wavenumber. The present results indicate it is unlikely this unknown ultraviolet physics can be described by a local perturbative effective field theory. Within the context of local effective field theory, one can still fine-tune the initial state so that it gives rise to unusual effects at the end of inflation. However, we now can convincingly argue that generic perturbations will inflate away and the unique de Sitter invariant Bunch-Davies state will be

left behind [1]. Up to fine tuning issues, the influence of high energy physics on inflation can then be captured by a local low-energy effective action analysis around the Bunch-Davies state, which leads to the conclusion that high energy physics corrections to the cosmic microwave background will typically be beyond the cosmic variance limits [67, 68] (notwithstanding some loop-holes [27, 28]). One can also view these results as highlighting the type of modification of conventional gravity needed to make sense of a variety of proposed trans-Planckian effects. Finally, it should also be noted our results do not apply to trans-Planckian corrections to inflation that do not asymptote to a de Sitter α-vacuum (see for example [96]).

Throwing theoretical objections to the four winds we explored some of the phenomenological consequences of the present universe being in an α-vacua. It seems the most promising way to directly detect a residual value for α today is via observations of ultra high energy cosmic rays. As we have mentioned, many of the predictions will be similar to production of ultra high energy cosmic rays via decaying super-heavy dark matter particles in the galactic halo [72, 18, 14]. See [17, 13, 88] for some recent results, and more extensive references. Let us briefly discuss some of the features and constraints on this production mechanism.

Galactic halo cosmic ray production avoids the GZK cutoff, because the absorption length of ultra high energy protons is of order 100 Mpc. The cosmic rays typically do not have time to scatter before they reach us, so the observed spectrum should reflect the fragmentation function of the primary decay. This has been computed using Monte Carlo

[1] One might hope that inflation was sufficiently short for certain pertubations to survive - see for example [66].

calculation in [13] including effects of supersymmetry. Perhaps the main problem one encounters in matching this with observation is that the fragmentation functions suggest the fraction of gamma rays versus protons is too high versus the experimental bound [10, 11, 86]. This bound should become much better established in the upcoming Pierre Auger Observatory [32]. It is possible gamma rays lose energy more efficiently than protons over the scales of interest, which would ameliorate this problem. Searches for ultra high energy neutrinos should provide a more robust test of this scenario.

The observed arrival directions of UHECRs exhibit a high degree of isotropy on large scales, but clustering on smaller scales. This can be consistent with a clumpy distribution of dark matter in the galactic halo. The α vacuum scenario predicts additional anisotropy if the coupling to visible and dark matter is comparable, but these couplings are not well-constrained given the current level of understanding.

The main goal of the present work was to investigate observational constraints on a residual value of α today. These constraints easily allow for the theoretically preferred value of $|e^{\alpha}| \sim H(t)/M_c$. It is fascinating the α vacua may also lead to a possible explanation of the spectrum of UHECRs.

Appendix A

Sundry matters

A.1 Squeezed states

We record some formulas useful in the manipulation of squeezed states.

$$\mathscr{U}(\zeta) \equiv \exp(\tfrac{1}{2}(\bar{\zeta}a^2 - \zeta a^{\dagger 2})) = e^A \tag{A.1.1}$$

$$e^A a e^{-A} = e^{\mathscr{L}_A} a \tag{A.1.2}$$

where $\mathscr{L}_A B \equiv [A,B]$. Let $\zeta = \rho e^{i\phi}$, then

$$\begin{aligned} [A,a] &= \zeta a^\dagger = \rho e^{i\phi} a^\dagger \\ &= \zeta^* a \,. \end{aligned} \tag{A.1.3}$$

This implies

$$\begin{aligned} \mathscr{L}_A^{2n+1} a &= e^{i\phi} \rho^{2n+1} a^\dagger \\ \mathscr{L}_A^{2n} a &= \rho^{2n} a \end{aligned} \tag{A.1.4}$$

so we obtain

$$\begin{aligned} e^A a e^{-A} &= a \sum \rho^{2n}/2n! + a^\dagger e^{i\phi} \sum \rho^{2n+1}/(2n+1)! \\ &= a_k \cosh(\rho) + a_k^\dagger e^{i\phi} \sinh(\rho) \end{aligned} \tag{A.1.5}$$

and

$$b_k = \mathscr{U} a_k \mathscr{U}^\dagger = N_\alpha (a_k - e^{\alpha^*} a_k^\dagger) = a_k \cosh(\rho) + a_k^\dagger e^{i\phi} \sinh(\rho) \; . \tag{A.1.6}$$

Some other expressions that we use:

$$e^{\alpha - \alpha^*} = e^{-2i\phi} : \phi = -\mathrm{Im}(\alpha) \tag{A.1.7}$$

$$e^{\alpha + \alpha^*} = \tanh^2 \rho \tag{A.1.8}$$

$$\begin{aligned} \rho &= \tanh^{-1} e^{\mathrm{Re}(\alpha)} \\ &= \tfrac{1}{2} \ln\left(\tfrac{1+e^{\mathrm{Re}(\alpha)}}{1-e^{\mathrm{Re}(\alpha)}}\right) \\ &= \tfrac{1}{2} \ln \tanh(-\tfrac{1}{2}\mathrm{Re}(\alpha)) \end{aligned} \tag{A.1.9}$$

$$\zeta = \tfrac{1}{2} e^{-i\mathrm{Im}(\alpha)} \ln \tanh(-\tfrac{1}{2}\mathrm{Re}(\alpha)) \; . \tag{A.1.10}$$

A.2 Some useful facts

Global coordinates

$$ds^2 = -dt^2 + \cosh^2 t d\Omega^2 \tag{A.2.1}$$

where $d\Omega^2$ is the metric on the unit 3-sphere. We will work in units where the Hubble radius is 1. Define Euclidean vacuum using mode functions

$$\psi_{klm}(x) = y_k(t) Y_{klm}(\Omega) \tag{A.2.2}$$

where k, l, m label the complete set of scalar spherical harmonics on S^3, $-|l| \leq m \leq |l|$. The $y_k(t)$ may be expressed in terms of the hypergeometric function ${}_2F_1$ [78]. These are regular on the Euclidean section, and may be analytically continued to functions regular on the lower half ζ plane, $\zeta = i \sinh t$. They have a branch cut from $\zeta = 1$ to $\zeta = \infty$.

Define linear combination

$$\phi_{klm} = \frac{e^{i\pi k/2}}{\sqrt{2}} \left(e^{i\pi/4} \psi_{klm}(x) + e^{-i\pi/4} \psi_{kl-m}(x) \right) \tag{A.2.3}$$

This set of modes is the basis of the complete set of modes we will use. They are orthonormal and positive norm, and satisfy

$$\begin{aligned} \phi_{klm}(\bar{x}) &= \phi^*_{klm}(x) \\ (\phi_{klm}, \phi_{k'l'm'}) &= \delta_{kk'} \delta_{ll'} \delta_{mm'} \end{aligned} \tag{A.2.4}$$

By definition the Euclidean vacuum Green function satisfies

$$G_E(x,y) = \sum_n \phi_n(x)\phi_n^*(y) \tag{A.2.5}$$

where we have compressed the k,l,m indices into the single index n.

It is useful to define $z(x,y) = X \cdot Y$ where X and Y are the coordinates of points on 5d Minkowski space, where de Sitter can be embedded as $-X_0^2 + X_1^2 + X_2^2 + X_3^2 + X_4^2 = 1$. For spacelike separations $z < 1$, for null separations $z = 1$, and for timelike separations $z > 1$. We have in mind continuing z to complex values for which the relation to geodesic distance breaks down. Note also that $z(\bar{x},y) = -z(x,y)$. In terms of z, (A.2.5) can be written explicitly as

$$G_E(x,y) = \frac{\Gamma(3/2+i\nu)\Gamma(3/2-i\nu)}{(4\pi)^2} {}_2F_1\left(3/2+i\nu, 3/2-i\nu, 2; (1+z)/2\right) \tag{A.2.6}$$

This function has a pole at $z = 1$ and a branch cut extending from $z = 1$ along the positive real axis. The function is analytic in the lower-half z plane. When z is real, $G_E(z)$ is real for $z < 1$, and develops an imaginary part for $z > 1$. The sign of this imaginary part changes as one moves across the branch cut.

To make (A.2.5) well-defined for time-like separations, we must specify an $i\varepsilon$ prescription. Near the singularity $z = 1$, we specify this in locally Minkowski coordinates $(t,\vec{x})$ by [20]

$$G_E(x,x') \sim \frac{1}{(t-t'-i\varepsilon)^2 - |\vec{x}-\vec{x}'|^2} \,. \tag{A.2.7}$$

In the text we introduce the Green functions $G_{ij}(x,y)$. These are likewise defined using

G_E but the $i\varepsilon$ prescriptions are as follows (for simplicity we set $\vec{x}$ and $\vec{x}'$ to 0):

$$G_{00}(x,x') = N_\alpha^2 G_E(t - i\varepsilon, t') \tag{A.2.8}$$

$$G_{10}(x,x') = N_\alpha^2 \gamma G_E(-t - i\varepsilon, t') \tag{A.2.9}$$

$$G_{01}(x,x') = N_\alpha^2 \gamma^* G_E(-t + i\varepsilon, t') \tag{A.2.10}$$

$$G_{11}(x,x') = N_\alpha^2 |\gamma|^2 G_E(t + i\varepsilon, t') \; . \tag{A.2.11}$$

Bibliography

[1] R. U. Abbasi et al. Measurement of the flux of ultrahigh energy cosmic rays from monocular observations by the high resolution fly's eye experiment. *Phys. Rev. Lett.*, 92:151101, 2004.

[2] A. A. Abrikosov, L. P. Gorkov, and I. E. Dzyaloshinski. Methods of quantum field theory in statistical physics. Dover Publications (1975).

[3] Stephen L. Adler. Massless, euclidean quantum electrodynamics on the five- dimensional unit hypersphere. *Phys. Rev.*, D6:3445–3461, 1972.

[4] Stephen L. Adler. Massless electrodynamics on the five-dimensional unit hypersphere: an amplitude - integral formulation. *Phys. Rev.*, D8:2400–2418, 1973.

[5] Gian Luigi Alberghi, Kevin Goldstein, and David A. Lowe. Ultra high energy cosmic rays and de sitter vacua. *Phys. Lett.*, B578:247–252, 2004.

[6] Bruce Allen. Vacuum states in de sitter space. *Phys. Rev.*, D32:3136, 1985.

[7] T. Altherr. Resummation of perturbation series in nonequilibrium scalar field theory. *Phys. Lett.*, B341:325–331, 1995.

[8] T. Altherr and D. Seibert. Problems of perturbation series in nonequilibrium quantum field theories. *Phys. Lett.*, B333:149–152, 1994.

[9] Luis Anchordoqui, Thomas Paul, Stephen Reucroft, and John Swain. Ultrahigh energy cosmic rays: The state of the art before the auger observatory. *Int. J. Mod. Phys.*, A18:2229–2366, 2003.

[10] M. Ave, J. A. Hinton, R. A. Vazquez, A. A. Watson, and E. Zas. New constraints from haverah park data on the photon and iron fluxes of uhe cosmic rays. *Phys. Rev. Lett.*, 85:2244–2247, 2000.

[11] M. Ave, J. A. Hinton, R. A. Vazquez, A. A. Watson, and E. Zas. Constraints on the ultra high energy photon flux using inclined showers from the haverah park array. *Phys. Rev.*, D65:063007, 2002.

[12] T. Banks and L. Mannelli. De sitter vacua, renormalization and locality. *Phys. Rev.*, D67:065009, 2003.

[13] Cyrille Barbot and Manuel Drees. Detailed analysis of the decay spectrum of a superheavy x particle. *Astropart. Phys.*, 20:5–44, 2003.

[14] Veniamin Berezinsky, Pasquale Blasi, and Alexander Vilenkin. Signatures of topological defects. *Phys. Rev.*, D58:103515, 1998.

[15] Lars Bergstrom and Ulf H. Danielsson. Can map and planck map planck physics? *JHEP*, 12:038, 2002.

[16] Denis Bernard and Antoine Folacci. Hadamard function, stress tensor and de sitter space. *Phys. Rev.*, D34:2286, 1986.

[17] Pijushpani Bhattacharjee and Gunter Sigl. Origin and propagation of extremely high energy cosmic rays. *Phys. Rept.*, 327:109–247, 2000.

[18] Michael Birkel and Subir Sarkar. Extremely high energy cosmic rays from relic particle decays. *Astropart. Phys.*, 9:297–309, 1998.

[19] N. D. Birrell and P. C. W. Davies. *Quatum fields in curved space*. Cambridge University Press, Cambrige, 1982. Cambridge, Uk: Univ. Pr. 340p.

[20] Raphael Bousso, Alexander Maloney, and Andrew Strominger. Conformal vacua and entropy in de sitter space. *Phys. Rev.*, D65:104039, 2002.

[21] Robert Brandenberger and Pei-Ming Ho. Noncommutative spacetime, stringy spacetime uncertainty principle, and density fluctuations. *Phys. Rev.*, D66:023517, 2002.

[22] Robert H. Brandenberger. Inflationary cosmology: Progress and problems. *Invited talk at IPM School on Cosmology 1999: Large Scale Structure Formation, Tehran, Iran, 23 Jan - 4 Feb 1999.*, 1999.

[23] Robert H. Brandenberger and Jerome Martin. The robustness of inflation to changes in super-planck- scale physics. *Mod. Phys. Lett.*, A16:999–1006, 2001.

[24] Robert H. Brandenberger and Jerome Martin. On signatures of short distance physics in the cosmic microwave background. *Int. J. Mod. Phys.*, A17:3663–3680, 2002.

[25] J. Bros, U. Moschella, and J. P. Gazeau. Quantum field theory in the de sitter universe. *Phys. Rev. Lett.*, 73:1746–1749, 1994.

[26] T. S. Bunch and P. C. W. Davies. Quantum field theory in de sitter space: Renormalization by point splitting. *Proc. Roy. Soc. Lond.*, A360:117–134, 1978.

[27] C. P. Burgess, J. M. Cline, and R. Holman. Effective field theories and inflation. *JCAP*, 0310:004, 2003.

[28] C. P. Burgess, J. M. Cline, F. Lemieux, and R. Holman. Are inflationary predictions sensitive to very high energy physics? *JHEP*, 02:048, 2003.

[29] E Calabi and L Markus. Relativistic space forms. *The Annals of Mathematics, 2nd Ser.*, 75:63–76, 1962.

[30] N. A. Chernikov and E. A. Tagirov. Quantum theory of scalar fields in de sitter space-time. *Annales Poincare Phys. Theor.*, A9:109, 1968.

[31] Hael Collins, R. Holman, and Matthew R. Martin. The fate of the alpha-vacuum. *Phys. Rev.*, D68:124012, 2003.

[32] J. W. Cronin. Summary of the workshop. *Nucl. Phys. Proc. Suppl.*, 28B:213–226, 1992.

[33] Ulf H. Danielsson. Inflation, holography and the choice of vacuum in de sitter space. *JHEP*, 07:040, 2002.

[34] Ulf H. Danielsson. A note on inflation and transplanckian physics. *Phys. Rev.*, D66:023511, 2002.

[35] Ulf H. Danielsson. On the consistency of de sitter vacua. *JHEP*, 12:025, 2002.

[36] B. S. Dewitt. Quantum field theory in curved space-time. *Phys. Rept.*, 19:295–357, 1975.

[37] J. S. Dowker and Raymond Critchley. Effective lagrangian and energy momentum tensor in de sitter space. *Phys. Rev.*, D13:3224, 1976.

[38] I. T. Drummond. Dimensional regularization of massless theories in spherical space-time. *Nucl. Phys.*, B94:115, 1975.

[39] I. T. Drummond. Conformally invariant amplitudes and field theory in a space-time of constant curvature. *Phys. Rev.*, D19:1123, 1979.

[40] I. T. Drummond and G. M. Shore. Conformal anomalies for interacting scalar fields in curved space-time. *Phys. Rev.*, D19:1134, 1979.

[41] I. T. Drummond and G. M. Shore. Dimensional regularization of massless quantum electrodynamics in spherical space-time. 1. *Ann. Phys.*, 117:89, 1979.

[42] Richard Easther, Brian R. Greene, William H. Kinney, and Gary Shiu. Inflation as a probe of short distance physics. *Phys. Rev.*, D64:103502, 2001.

[43] Richard Easther, Brian R. Greene, William H. Kinney, and Gary Shiu. A generic estimate of trans-planckian modifications to the primordial power spectrum in inflation. *Phys. Rev.*, D66:023518, 2002.

[44] Richard Easther, Brian R. Greene, William H. Kinney, and Gary Shiu. Imprints of short distance physics on inflationary cosmology. *Phys. Rev.*, D67:063508, 2003.

[45] Martin B. Einhorn and Finn Larsen. Interacting quantum field theory in de sitter vacua. *Phys.Rev.*, D67:024001, 2003.

[46] Martin B. Einhorn and Finn Larsen. Squeezed states in the de sitter vacuum. *Phys.Rev.*, D68:064002, 2003.

[47] T. . S. Evans and A. C. Pearson. A reexamination of the path ordered approach to real time thermal field theory. *Phys. Rev.*, D52:4652–4659, 1995.

[48] T. S. Evans. Spectral representation of three point functions at finite temperature. *Phys. Lett.*, B252:108–112, 1990.

[49] T. S. Evans. N point finite temperature expectation values at real times. *Nucl. Phys.*, B374:340–372, 1992.

[50] T. S. Evans. What is being calculated with thermal field theory? *Talk given at Lake Louise Winter Institute: Particle Physics and Cosmology, Lake Louise, Canada, 20-26 Feb 1994. Published in Lake Louise Winter Inst.1994:0343-352*, 1994.

[51] R. Floreanini, C. T. Hill, and R. Jackiw. Functional representation for the isometries of de sitter space. *Ann. Phys.*, 175:345, 1987.

[52] J. P. Gazeau, J. Renaud, and M. V. Takook. Gupta-bleuler quantization for minimally coupled scalar fields in de sitter space. *Class. Quant. Grav.*, 17:1415–1434, 2000.

[53] J. Géhéniau and C. Schomblond. *Acad. R. Belg. Bull. Cl. Sci.*, 54:1147, 1968.

[54] Kevin Goldstein and David A. Lowe. Initial state effects on the cosmic microwave background and trans-planckian physics. *Phys. Rev.*, D67:063502, 2003.

[55] Kevin Goldstein and David A. Lowe. A note on alpha-vacua and interacting field theory in de sitter space. *Nucl. Phys.*, B669:325–340, 2003.

[56] Kevin Goldstein and David A. Lowe. Real-time perturbation theory in de sitter space. *Phys. Rev.*, D69:023507, 2004.

[57] O. W. Greenberg. Cpt violation implies violation of lorentz invariance. *Phys. Rev. Lett.*, 89:231602, 2002.

[58] Kenneth Greisen. End to the cosmic ray spectrum? *Phys. Rev. Lett.*, 16:748–750, 1966.

[59] F. Guerin. Retarded - advanced n point green functions in thermal field theories. *Nucl. Phys.*, B432:281–314, 1994.

[60] S. W. Hawking. Interacting quantum fields around a black hole. *Commun. Math. Phys.*, 80:421, 1981.

[61] S. W. Hawking. The unpredictability of quantum gravity. *Commun. Math. Phys.*, 87:395, 1982.

[62] S. W. Hawking. The chronology protection conjecture. *Phys. Rev.*, D46:603–611, 1992.

[63] S. W. Hawking and G. F. R. Ellis. *Large Scale Structure of Space-Time*. Cambridge University Press, Cambrige, 1973.

[64] N. Hayashida et al. Observation of a very energetic cosmic ray well beyond the predicted 2.7-k cutoff in the primary energy spectrum. *Phys. Rev. Lett.*, 73:3491–3494, 1994.

[65] A. Houriet and A. Kind. Classification invariante des termes de la matrice s. *Helv. Phys. Acta*, 22:319, 1949.

[66] Nemanja Kaloper and Manoj Kaplinghat. Primeval corrections to the cmb anisotropies. 2003.

[67] Nemanja Kaloper, Matthew Kleban, Albion Lawrence, Stephen Shenker, and Leonard Susskind. Initial conditions for inflation. *JHEP*, 11:037, 2002.

[68] Nemanja Kaloper, Matthew Kleban, Albion E. Lawrence, and Stephen Shenker. Signatures of short distance physics in the cosmic microwave background. *Phys. Rev.*, D66:123510, 2002.

[69] J. I. Kapusta. Finite temperature field theory. Cambridge, Uk: Univ. Pr. (1989).

[70] Bernard S. Kay and Robert M. Wald. Theorems on the uniqueness and thermal properties of stationary, nonsingular, quasifree states on space-times with a bifurcate killing horizon. *Phys. Rept.*, 207:49–136, 1991.

[71] Achim Kempf and Jens C. Niemeyer. Perturbation spectrum in inflation with cutoff. *Phys. Rev.*, D64:103501, 2001.

[72] V. A. Kuzmin and V. A. Rubakov. Ultrahigh-energy cosmic rays: A window on postinflationary reheating epoch of the universe? *Phys. Atom. Nucl.*, 61:1028–1030, 1998.

[73] N. P. Landsman and C. G. van Weert. Real and imaginary time field theory at finite temperature and density. *Phys. Rept.*, 145:141, 1987.

[74] Fedele Lizzi, Gianpiero Mangano, Gennaro Miele, and Marco Peloso. Cosmological perturbations and short distance physics from noncommutative geometry. *JHEP*, 06:049, 2002.

[75] David A. Lowe, Joseph Polchinski, Leonard Susskind, Larus Thorlacius, and John Uglum. Black hole complementarity versus locality. *Phys. Rev.*, D52:6997–7010, 1995.

[76] Jerome Martin and Robert H. Brandenberger. The trans-planckian problem of inflationary cosmology. *Phys. Rev.*, D63:123501, 2001.

[77] Jerome Martin and Robert H. Brandenberger. The corley-jacobson dispersion relation and trans-planckian inflation. *Phys. Rev.*, D65:103514, 2002.

[78] E. Mottola. Particle creation in de sitter space. *Phys. Rev.*, D31:754, 1985.

[79] Jens C. Niemeyer, Renaud Parentani, and David Campo. Minimal modifications of the primordial power spectrum from an adiabatic short distance cutoff. *Phys. Rev.*, D66:083510, 2002.

[80] A. J. Niemi and G. W. Semenoff. Finite temperature quantum field theory in minkowski space. *Ann. Phys.*, 152:105, 1984.

[81] Maulik K. Parikh, Ivo Savonije, and Erik Verlinde. Elliptic de sitter space: ds/z(2). *Phys. Rev.*, D67:064005, 2003.

[82] H. V. Peiris et al. First year wilkinson microwave anisotropy probe (wmap) observations: Implications for inflation. *Astrophys. J. Suppl.*, 148:213, 2003.

[83] Adam G. Riess. The case for an accelerating universe from supernovae. *Publ. Astron. Soc. Pac.*, 112:1284, 2000.

[84] Gordon W. Semenoff and Nathan Weiss. Feynman rules for finite temperature green's functions in an expanding universe. *Phys. Rev.*, D31:689, 1985.

[85] S. Shankaranarayanan. Is there an imprint of planck scale physics on inflationary cosmology? *Class. Quant. Grav.*, 20:75–84, 2003.

[86] K. Shinozaki et al. Upper limit on gamma-ray flux above 10**19-ev estimated by the akeno giant air shower array experiment. *Astrophys. J.*, 571:L117–L120, 2002.

[87] E Shrödinger. *Expanding Universes*. Cambridge University Press, London, 1956.

[88] Guenter Sigl. The enigma of the highest energy particles of nature. *Ann. Phys.*, 303:117–141, 2003.

[89] Marcus Spradlin, Andrew Strominger, and Anastasia Volovich. Les houches lectures on de sitter space. *Prepared for Les Houches Summer School: Session 76: Euro Summer School on Unity of Fundamental Physics: Gravity, Gauge Theory and Strings,*

*Les Houches, France, 30 Jul - 31 Aug 2001. Published in *Les Houches 2001, Gravity, gauge theories and strings* 423-453*, 2001.

[90] Alexei A. Starobinsky. Robustness of the inflationary perturbation spectrum to trans-planckian physics. *Pisma Zh. Eksp. Teor. Fiz.*, 73:415–418, 2001.

[91] Alexei A. Starobinsky and Igor I. Tkachev. Trans-planckian particle creation in cosmology and ultra- high energy cosmic rays. *JETP Lett.*, 76:235–239, 2002.

[92] K. Svozil. Quantum electrodynamics in the squeezed vacuum state: Feynman rules and corrections to the electron mass and anomalous magnetic moment. 1994.

[93] E. A. Tagirov. Consequences of field quantization in de sitter type cosmological models. *Ann. Phys.*, 76:561–579, 1973.

[94] Yasushi Takahasi and Hiroomi Umezawa. Thermo field dynamics. *Collect. Phenom.*, 2:55–80, 1975.

[95] M. Takeda et al. Extension of the cosmic-ray energy spectrum beyond the predicted greisen-zatsepin-kuzmin cutoff. *Phys. Rev. Lett.*, 81:1163–1166, 1998.

[96] Shinji Tsujikawa, Roy Maartens, and Robert Brandenberger. Non-commutative inflation and the cmb. *Phys. Lett.*, B574:141–148, 2003.

[97] R. M. Wald. Quantum field theory in curved space-time and black hole thermodynamics. Chicago, USA: Univ. Pr. (1994) 205 p.

[98] G. C. Wick. The evaluation of the collision matrix. *Phys. Rev.*, 80:268–272, 1950.

[99] G. T. Zatsepin and V. A. Kuzmin. Upper limit of the spectrum of cosmic rays. *JETP Lett.*, 4:78–80, 1966.